

1 **An analytical** model for simulating two-dimensional multispecies plume
2 **migration**

3
4 Jui-Sheng Chen^a, Ching-Ping Liang^b, Chen-Wuing Liu^{c,*}, Loretta Y. Li^d

5
6 ^a*Graduate Institute of Applied Geology, National Central University, Jhongli, Taoyuan 32001,*

7 *Taiwan*

8 ^b*Department of Environmental Engineering and Science, Fooyin University, Kaohsiung 83101,*

9 *Taiwan*

10 ^c*Department of Bioenvironmental Systems Engineering, National Taiwan University, Taipei 10617,*

11 *Taiwan*

12 ^d*Department of Civil Engineering, University of British Columbia, Vancouver, BC V6T 1Z4,*

13 *Canada*

14
15 *Corresponding author: *Chen-Wuing Liu, Department of Bioenvironmental Systems Engineering,*
16 *National Taiwan University, Taipei 10617, Taiwan*

17 E-mail: cwliu@ntu.edu.tw

18 Tel: +886-2-23626480

23 **Abstract**

24 The two-dimensional advection-dispersion equations coupled with sequential first-order decay
25 reactions involving arbitrary number of species in groundwater system is considered to predict the
26 two-dimensional plume behavior of decaying contaminant such as radionuclide and dissolved
27 chlorinated solvent. Generalized analytical solutions in compact format are derived through the
28 sequential application of the Laplace, finite Fourier cosine, and generalized integral transform to
29 reduce the coupled partial differential equation system to a set of linear algebraic equations. The
30 system of algebraic equations is next solved for each species in the transformed domain, and the
31 solutions in the original domain are then obtained through consecutive integral transform inversions.
32 Explicit form solutions for a special case are derived using the generalized analytical solutions and
33 are compared with the numerical solutions. The analytical results indicate that the analytical solutions
34 are robust, accurate and useful for simulation or screening tools to assess plume behaviors of decaying
35 contaminants.

36

37 *Keywords:* Parsimonious analytical model; reactive transport; first-order decay reaction; Bateman-
38 type source; radionuclide; dissolved chlorinated solvent.

39

40 **1. Introduction**

41 Experimental and theoretical studies have been undertaken to understand the fate and transport of
42 dissolved hazardous substances in subsurface environments because that human health is threatened
43 by a wide spectrum of contaminants in groundwater and soil. Analytical models are essential and
44 efficient tools for understanding pollutants behavior in subsurface environments. Several analytical
45 solutions for single-species transport problems have been reported for simulating the transport of
46 various contaminants (Batu, 1989; 1993; 1996; Chen et al., 2008a; 2008b; 2011; Gao et al., 2010; 2012;
47 2013; Leij et al., 1991; 1993; Park and Zhan, 2001; Pérez Guerrero and Skaggs, 2010 ; Pérez Guerrero
48 et al., 2013 ; van Genuchten and Alves, 1982; Yeh, 1981; Zhan et al., 2009; Ziskind et al., 2011).
49 Transport processes of some contaminants such as radionuclides, dissolved chlorinated solvents and
50 nitrogen generally involve a series of first-order or pseudo first-order sequential decay chain reactions.
51 During migrations of decaying contaminants, mobile and toxic successor products may sequentially
52 form and move downstream with elevated concentrations. Single-species analytical models do not
53 permit transport behaviors of successor species of these decaying contaminants to be evaluated.
54 Analytical models for multispecies transport equations coupled with first-order sequential decay
55 reactions are useful tools for synchronous determination of the fate and transport of the predecessor
56 and successor species of decaying contaminants. However, there are few analytical solutions for
57 coupled multispecies transport equations compared to a large body of analytical solutions in the
58 literature pertaining to the single-species advective-dispersive transport subject to a wide spectrum of
59 initial and boundary conditions.

60 Mathematical approaches have been proposed in the literature to derive a limited number of one-
61 dimensional analytical solutions or semi-analytical solutions for multispecies advective–dispersive
62 transport equations sequentially coupled with first-order decay reactions. These include direct integral
63 transforms with sequential substitutions (Cho, 1971; Lunn et al., 1996; van Genuchten, 1985, Mieleles

64 and Zhan, 2012), decomposition by change-of-variables with the help of existing single-species
65 analytical solutions (Sun and Clement, 1999; Sun et al., 1999a; 1999b), Laplace transform combined
66 with decomposition of matrix diagonalization (Quezada et al., 2004; Srinivasan and Clement, 2008a;
67 2008b), decomposition by change-of-variables coupled with generalized integral transform (Pérez
68 Guerrero et al., 2009; 2010), sequential integral transforms in association with algebraic decomposition
69 (Chen et al., 2012a; 2012b).

70 Multi-dimensional solutions are needed for real world applications, making them more attractive
71 than one-dimensional solutions. Bauer et al. (2001) presented the first set of semi-analytical solutions
72 for one-, two-, and three-dimensional coupled multispecies transport problem with distinct retardation
73 coefficients. Explicit analytical solutions were derived by Montas (2003) for multi-dimensional
74 advective-dispersive transport coupled with first-order reactions for a three-species transport system
75 with distinct retardation coefficients of species. Quezada et al. (2004) extended the Clement (2001)
76 strategy to obtain Laplace-domain solutions for an arbitrary decay chain length. Most recently, Sudicky
77 et al. (2013) presented a set of semi-analytical solutions to simulate the three-dimensional multi-
78 species transport subject to first-order chain-decay reactions involving up to seven species and four
79 decay levels. Basically, their solutions were obtained species by species using recursion relations
80 between target species and its predecessor species. For a straight decay chain, they derived solutions
81 for up to four species and no generalized expressions with compact formats for any target species were
82 obtained. Note that their solutions were derived for the first-type (Dirichlet) inlet conditions which
83 generally bring about physically improper mass conservation and significant errors in predicting the
84 concentration distributions especially for a transport system with a large longitudinal dispersion
85 coefficient (Barry and Sposito, 1988; Parlange et al., 1992). Moreover, in addition to some special
86 cases, the numerical Laplace transforms are required to obtain the original time domain solution.
87 Besides the straight decay chain, the analytical model by Clement (2001) and Sudicky (2013) can

88 account for more complicated decay chain problems such as diverging, converging and branched decay
89 chains.

90 Based on the aforementioned reviews, this study presents a parsimonious explicit analytical model
91 for two-dimensional multispecies transport coupled by a series of first-order decay reactions involving
92 an arbitrary number of species in groundwater system. The derived analytical solutions have four
93 salient features. First, the third-type (Robin) inlet boundary conditions which satisfy mass conservation
94 are considered. Second, the solution is explicit, thus solution can be easily evaluated without invoking
95 the numerical Laplace inversion. Third, the generalized solutions with parsimonious mathematical
96 structures are obtained and valid for any species of a decay chain. The parsimonious mathematical
97 structures of the generalized solutions are easy to code into a computer program for implementing the
98 solution computations for arbitrary target species. Fourth, the derived solutions can account for any
99 decay chain length. The explicit analytical solutions have applications for evaluation of concentration
100 distribution of arbitrary target species of the real-world decaying contaminants. The developed
101 parsimonious model is robustly verified with three example problems and applied to simulate the
102 multispecies plume migration of dissolved radionuclides and chlorinated solvent.

103

104 **2. Governing equations and analytical solutions**

105 *2.1 Derivation of analytical solutions*

106 This study consider the problem of decaying contaminant plume migration. The source zone is
107 located in the upstream of groundwater flow. The source zone can represent leaching of radionuclide
108 from a radioactive waste disposal facility or release of chlorinated solvent from the residual NAPL
109 phase into the aqueous phase. After these decaying contaminants enter the aqueous phase, they migrate
110 by one-dimensional advection with flowing groundwater and by simultaneously longitudinal and
111 transverse dispersion processes. While migrating in the groundwater system, the contaminants undergo

112 linear isothermal equilibrium sorption and a series of sequential first-order decaying reactions. Sudicky
 113 et al. (2013) provided the detailed modeling scenario. The scenario considered in this study can be
 114 ideally described as shown in Fig. 1. A steady and uniform velocity in the x direction is considered
 115 in Fig. 1. The governing equations describing two-dimensional reactive transport of the decaying
 116 contaminants and their successor species undergoing linear isothermal equilibrium sorption and a series
 117 of sequential first-order decaying reactions can be mathematically written as

$$118 \quad D_L \frac{\partial^2 C_1(x, y, t)}{\partial x^2} - v \frac{\partial C_1(x, y, t)}{\partial x} + D_T \frac{\partial^2 C_1(x, y, t)}{\partial y^2} - k_1 R_1 C_1(x, y, t) \quad (1a)$$

$$= R_1 \frac{\partial C_1(x, y, t)}{\partial t}$$

$$119 \quad D_L \frac{\partial^2 C_i(x, y, t)}{\partial x^2} - v \frac{\partial C_i(x, y, t)}{\partial x} + D_T \frac{\partial^2 C_i(x, y, t)}{\partial y^2} - k_i R_i C_i(x, y, t) \quad i = 2 \dots N. \quad (1b)$$

$$+ k_{i-1} R_{i-1} C_{i-1}(x, y, t) = R_i \frac{\partial C_i(x, y, t)}{\partial t}$$

120 where $C_i(x, y, t)$ is the aqueous concentration of species i [\mathbf{ML}^{-3}]; x and y are the spatial
 121 coordinates in the groundwater flow and perpendicular directions [\mathbf{L}], respectively; t is time [\mathbf{T}];
 122 D_L and D_T represent the longitudinal and transverse dispersion coefficients [$\mathbf{L}^2\mathbf{T}^{-1}$], respectively;
 123 v is the average steady and uniform pore-water velocity [\mathbf{LT}^{-1}]; k_i is the first-order decay rate
 124 constant of species i [\mathbf{T}^{-1}]; R_i is the retardation coefficient of species i [-]. Note that these equations
 125 consider that the decay reactions occur simultaneously in both the aqueous and sorbed phases. If the
 126 decay reactions occur only in the aqueous phase, the retardation coefficients in the decay terms in the
 127 right-hand sides of Eqs. (1a) and (1b) become unity. For such case, k_i and k_{i-1} in the left-hand sides
 128 could be modified as $\frac{k_i}{R_i}$ and $\frac{k_{i-1}}{R_{i-1}}$ to facilitate the application of the derived analytical solutions
 129 obtained by Eqs. (1a) and (1b).

130 The initial and boundary conditions for solving Eqs. (1a) and (1b) are:

131 $C_i(x, y, t = 0) = 0 \quad 0 \leq x \leq L, 0 \leq y \leq W \quad i = 1 \dots N.$ (2)

132 $-D_L \frac{\partial C_i(x=0, y, t)}{\partial x} + vC_i(x=0, y, t) = vf_i(t)[H(y - y_1) - H(y - y_2)] \quad t \geq 0 \quad i = 1 \dots N.$ (3)

133 $\frac{\partial C_i(x=L, y, t)}{\partial x} = 0 \quad t \geq 0, 0 \leq y \leq W \quad i = 1 \dots N.$ (4)

134 $\frac{\partial C_i(x, y=0, t)}{\partial y} = 0 \quad t \geq 0, 0 \leq x \leq L \quad i = 1 \dots N.$ (5)

135 $\frac{\partial C_i(x, y=W, t)}{\partial y} = 0 \quad t \geq 0, 0 \leq x \leq L \quad i = 1 \dots N.$ (6)

136 where $f_i(t)$ is the arbitrary time-dependent source concentration of species i applied at the source
137 segment ($H(y - y_1) - H(y - y_2)$) at boundary ($x = 0$) which will be specified later [L], $H(\bullet)$ is the
138 Heaviside function, L and W are the length and width of the transport system under consideration
139 [L]. Eq. (2) implies that the transport system is free of solute mass at the initial time.

140 Eq. (3) means that a third-type boundary condition satisfying mass conservation at the inlet boundary
141 is considered. Eq. (4) considers the concentration gradient to be zero at the exit boundary based on
142 the mass conservation principle. Such a boundary condition has been widely used for simulating
143 solute transport in a finite-length system. Eqs. (5) and (6) **assume** no solute flux across the lower and
144 upper boundaries. It is noted that in Eq. (3), we assume arbitrary time-dependent sources of species i
145 uniformly distributed at the segment ($y_1 \leq y \leq y_2$) of the inlet boundary ($x = 0$), the so-called
146 Heaviside function source concentration profile. Relative to the first type boundary conditions used
147 by Sudicky et al. (2013), the third-type boundary conditions which satisfy mass conservation at the
148 inlet boundary (Barry and Sposito, 1988; Parlange et al., 1992) are used herein. Sudicky et al. (2013)
149 considered the source concentration profiles as Gaussian or Heaviside step functions. If Gaussain
150 distributions are desired, we can easily replace the Heaviside function in the right-hand side of Eq.

151 (3) with a Gaussian distribution.

152 Eqs. (1)-(6) can be expressed in dimensionless form as

$$153 \quad \frac{1}{Pe_L} \frac{\partial^2 C_1(X,Y,Z)}{\partial X^2} - \frac{\partial C_1(X,Y,Z)}{\partial X} + \frac{\rho^2}{Pe_T} \frac{\partial^2 C_1(X,Y,Z)}{\partial Y^2} - \kappa C_1(X,Y,Z) = R_1 \frac{\partial C_1(X,Y,T)}{\partial T} \quad (7a)$$

$$154 \quad \frac{1}{Pe_L} \frac{\partial^2 C_i(X,Y,T)}{\partial X^2} - \frac{\partial C_i(X,Y,T)}{\partial X} + \frac{\rho^2}{Pe_T} \frac{\partial^2 C_i(X,Y,T)}{\partial Y^2} \quad i = 2 \dots N. \quad (7b)$$

$$- \kappa_i C_i(X,Y,T) + \kappa_{i-1} C_{i-1}(X,Y,T) = R_i \frac{\partial C_i(X,Y,T)}{\partial T}$$

$$155 \quad C_i(X,Y,T=0) = 0 \quad 0 \leq X \leq 1, 0 \leq Y \leq 1 \quad i = 1 \dots N. \quad (8)$$

$$156 \quad - \frac{1}{Pe_L} \frac{\partial C_i(X=0,Y,T)}{\partial X} + C_i(X=0,Y,Z) = f_i(T) [H(Y-Y_1) - H(Y-Y_2)] \quad T \geq 0, i = 1 \dots N. \quad (9)$$

$$157 \quad \frac{\partial C_i(X=1,Y,T)}{\partial X} = 0 \quad T \geq 0, 0 \leq Y \leq 1 \quad i = 1 \dots N. \quad (10)$$

$$158 \quad \frac{\partial C_i(X,Y=0,T)}{\partial Y} = 0 \quad T \geq 0, 0 \leq X \leq 1 \quad i = 1 \dots N. \quad (11)$$

$$159 \quad \frac{\partial C_i(X,Y=1,T)}{\partial Y} = 0 \quad T \geq 0, 0 \leq X \leq 1 \quad i = 1 \dots N. \quad (12)$$

$$160 \quad \text{where } X = \frac{x}{L}, Y = \frac{y}{W}, Y_1 = \frac{y_1}{W}, Y_2 = \frac{y_2}{W}, T = \frac{vt}{L}, Pe_L = \frac{vL}{D_L}, Pe_T = \frac{vL}{D_T}, \rho = \frac{L}{W}.$$

161 Our solution strategy used is extended from the approach proposed by Chen et al. (2012a; 2012b).

162 The core of this approach is that the coupled partial differential equations are converted into an
 163 algebraic equation system via a series of integral transforms and the solutions in the transformed
 164 domain for each species are directly and algebraically obtained by sequential substitutions.

165 Following Chen et al. (2012a; 2012b), the generalized analytical solutions in compact formats can
 166 be obtained as follows (with detailed derivation provided in Appendix A)

$$\begin{aligned}
& C_i(X, Y, T) \\
167 \quad & = f_i(T)\Phi(n=0) + e^{\frac{Pe_L X}{2}} \sum_{l=1}^{\infty} \frac{K(\xi_l, X)}{N(\xi_l)} [p_i(\xi_l, n, T) + q_i(\xi_l, n, T)]\Phi(n=0)\Theta(\xi_l) \quad (13) \\
& + 2 \sum_{n=1}^{n=\infty} \left\{ f_i(T)\Phi(n) + e^{\frac{Pe_L X}{2}} \sum_{l=1}^{\infty} \frac{K(\xi_l, X)}{N(\xi_l)} [p_i(\xi_l, n, T) + q_i(\xi_l, n, T)]\Phi(n)\Theta(\xi_l) \right\} \cos(n\pi Y)
\end{aligned}$$

$$168 \quad \text{where } \Phi(n) = \begin{cases} Y_2 - Y_1 & n = 0 \\ \frac{\sin(n\pi Y_2) - \sin(n\pi Y_1)}{n\pi} & n = 1, 2, 3, \dots \end{cases}, \quad \xi_l \text{ is the eigenvalue, determined from the}$$

$$169 \quad \text{equation } \xi_l \cot \xi_l - \frac{\xi_l^2}{Pe_L} + \frac{Pe_L}{4} = 0, \quad \Theta(\xi_l) = \frac{Pe_L \xi_l}{\frac{Pe_L^2}{4} + \xi_l^2}, \quad K(\xi_l, X) = \frac{Pe_L}{2} \sin(\xi_l X) + \xi_l \cos(\xi_l X),$$

$$170 \quad N(\xi_l) = \frac{2}{\frac{Pe_L^2}{4} + Pe_L + \xi_l^2},$$

$$171 \quad p_i(\xi_l, n, T) = f_i(T) - \beta_i e^{-\alpha_i T} \int_0^T f_i(\tau) e^{\alpha_i \tau} d\tau \quad (14)$$

172 and

$$173 \quad q_i(\xi_l, n, T) = \sum_{k=0}^{k=i-2} \left(\beta_{i-k-1} \prod_{j_1=0}^{j_1=k} \sigma_{i-j_1} \right) \sum_{j_2=0}^{j_2=k+1} \frac{e^{-\alpha_{i-j_2} T} \int_0^T e^{\alpha_{i-j_2} \tau} f_{i-k-1}(\tau) d\tau}{\prod_{\substack{j_3=i \\ j_3=i-k-1, j_3 \neq i-j_2}} (\alpha_{j_3} - \alpha_{i-j_2})} \quad (15)$$

$$174 \quad \text{where } \alpha_i(\xi_l) = \frac{\kappa_i}{R_i} + \frac{\rho^2 n^2 \pi^2}{Pe_T R_i} + \frac{Pe_L}{4R_i} + \frac{\xi_l^2}{Pe_L R_i}, \quad \beta_i(\xi_l) = \frac{Pe_L}{4R_i} + \frac{\xi_l^2}{Pe_L R_i}, \quad \sigma_i = \frac{\kappa_{i-1}}{R_i}$$

175 Concise expressions for arbitrary target species such as described in Eqs. (13) to (15) facilitate the
176 development of a computer code for implementing the computations of the analytical solutions.

177 The generalized solutions of Eq. (13) accompanied by two corresponding auxiliary functions

178 $p_i(\xi_l, n, T)$ and $q_i(\xi_l, n, T)$ in Eqs. (14)-(15) can be applied to derive analytical solutions for some

179 special-case inlet boundary sources. Here the time-dependent decaying source which represents the
 180 specific release mechanism defined by the Bateman equations (van Genuchten, 1985) is considered.
 181 A Bateman-type source is described by

$$182 \quad f_i(t) = \sum_{m=1}^i b_{im} e^{-\delta_m t} \quad (16a)$$

183 or in dimensionless form,

$$184 \quad f_i(T) = \sum_{m=1}^{m=i} b_{im} e^{-\lambda_m T} \quad (16b)$$

185 The coefficients b_{im} and $\delta_m = \mu_m + \gamma_m$ account for the first-order decay reaction rate (μ_m) of each
 186 species in the waste source and the release rate (γ_m) of each species from the waste source,

$$187 \quad \lambda_m = \frac{\delta_m L}{v}.$$

188 By substituting Eq. (16b) into Eqs. (13)-(15), we obtain

$$189 \quad \begin{aligned} & C_i(X, Y, T) \\ &= \sum_{m=1}^{m=i} b_{im} e^{-\lambda_m T} \Phi(n=0) + e^{\frac{Pe_L X}{2}} \sum_{l=1}^{\infty} \frac{K(\xi_l, X)}{N(\xi_l)} [p_i(\xi_l, n, T) + q_i(\xi_l, n, T)] \Phi(n=0) \Theta(\xi_l) \\ &+ 2 \sum_{n=1}^{n=\infty} \left\{ \sum_{m=1}^{m=i} b_{im} e^{-\lambda_m T} \Phi(n) + e^{\frac{Pe_L X}{2}} \sum_{l=1}^{\infty} \frac{K(\xi_l, X)}{N(\xi_l)} [p_i(\xi_l, n, T) + q_i(\xi_l, n, T)] \Phi(n) \Theta(\xi_l) \right\} \cos(n\pi Y) \end{aligned} \quad (17)$$

191 where

$$192 \quad p_i(\xi_l, n, T) = \sum_{m=1}^{m=i} b_{i,m} \cdot e^{-\lambda_m T} - \beta_i \sum_{m=1}^{m=i} b_{i,m} \frac{e^{-\lambda_m T} - e^{-\alpha_i T}}{\alpha_i - \lambda_m} \quad (18)$$

193 and

194
$$p_i(\xi_l, n, T) = \sum_{k=0}^{k=i-2} \left(\beta_{i-k-1} \prod_{j_1=0}^{j_1=k} \sigma_{i-j_1} \right) \sum_{j_2=0}^{j_2=k+1} \frac{\sum_{m=1}^{m=i-k-1} \frac{b_{i-k-1,m} \left(e^{-\lambda_m T} - e^{-\alpha_{i-j_2} T} \right)}{\alpha_{i-j_2} - \lambda_m}}{\prod_{j_3=i-k-1, j_3 \neq i-j_1}^{j_3=i} (\alpha_{j_3} - \alpha_{i-j_2})} \quad (19)$$

195

196 **2.2 Convergence behavior of the Bateman-type source solution**

197 Based on the special-case analytical solutions in Eq. (17) supported by two auxiliary functions,
 198 defined in Eqs. (18) and (19), a computer code was developed in FORTRAN 90 language with double
 199 precision. The details of the FORTRAN computer code are described in Supplement. The derived
 200 analytical solutions in Eqs. (17)-(19) consist of summations of double infinite series expansions for
 201 the finite Fourier cosine and generalized integral transform inversions, respectively. It is
 202 straightforward to sum up these two infinite series expansions term by term. To avoid time-consuming
 203 summations of these infinite series expansions, the convergence tests should be routinely executed to
 204 determine the optimal number of the required terms for evaluating analytical solutions to the desired
 205 accuracies. Two-dimensional four-member radionuclide decay chain
 206 $^{238}\text{Pu} \rightarrow ^{234}\text{U} \rightarrow ^{230}\text{Th} \rightarrow ^{226}\text{Ra}$ is considered herein as convergence test example 1 to demonstrate
 207 the convergence behavior of the series expansions. This convergence test example 1 is modified from
 208 a one-dimensional radionuclide decay chain problem originated by Higashi and Pigford (1980) and
 209 later applied by van Genuchten (1985) to illustrate the applicability of their derived solution. The
 210 important model parameters related to this test example are listed in Tables 1 and 2. The inlet source
 211 is chosen to be symmetrical with respect to the x -axis and conveniently arranged in the
 212 $40\text{ m} \leq y \leq 60\text{ m}$ segment at the inlet boundary.

213 In order to determine the optimal term number of series expansions for the finite Fourier cosine
 214 transform inverse to achieve accurate numerical evaluation, we specify a sufficiently large number of

215 series expansions for the generalized transform inverse so that the influence of the number of series
216 expansions for the generalized integral transform inverse on convergence of series expansion for finite
217 Fourier cosine transform inverse can be excluded. A similar concept is used when investigating the
218 required number of terms in the series expansions for the generalized integral transform inverse. An
219 alternative approach is conducted by simultaneously varying the term numbers of series expansions
220 for the generalized integral transform inverse and the finite Fourier cosine transform inverse.

221 Tables 3, 4 and 5 give results of the convergence tests up to 3 decimal digits of the solution
222 computations along the three transects (inlet boundary at $x=0$ m, $x=25$ m, and exit boundary at x
223 $=250$ m). In these tables M and N are defined as the numbers of terms summed for the generalized
224 integral transform inverse and finite Fourier cosine transform inverse, respectively. It is observed that
225 M and N are related closely to the true values of the solutions. For smaller true values, the solutions
226 must be computed with greater M and N . However, convergences can be drastically speeded up if
227 lower calculation precision (e.g. 2 decimal digits accuracy) is acceptable. For example,
228 $(M, N) = (100, 200)$ is sufficient for 2 decimal digits accuracy, while for 3 decimal digits accuracy we
229 need $(M, N) = (1600, 8000)$. Two decimal digits accuracy is acceptable for most practical problems.
230 It is also found that M increases and N decreases with increasing x .

231 To further examine the series convergence behavior, example 2 considers a transport system of
232 large aspect ratio ($\frac{L}{W} = \frac{2,500m}{100m}$) and a narrower source segment, $45 m \leq y \leq 55 m$, on the inlet
233 boundary. Tables 6 and 7 present results of the convergence tests of the solution computations along
234 two transects (inlet boundary and $x=250$ m). Tables 6 and 7 also show similar results for the
235 dependences of M and N on x . Note that larger M and N are required for each species in this
236 test example, suggesting that the evaluation of the solution for a large aspect ratio requires more series
237 expansion terms to achieve the same accuracy as compared to example 1. Detailed results of the

238 convergence test examples 1 and 2 are provided in Supplement.

239 Using the required numbers determined from the convergence test, the computational time for
240 evaluation of the solutions at 50 different observations only takes 3.782s, 11.325s, 23.95s and 67.23s
241 computer clock time on an Intel Core i7-2600 3.40 MHz PC for species 1, 2, 3, and 4 in the comparison
242 of example 1.

243

244 **3. Results and discussion**

245 *3.1 Comparison of the analytical solutions with the numerical solutions*

246 Three comparison examples are considered to examine the correctness and robustness of the
247 analytical solutions and the accuracy of the computer code. The first comparison example is the four-
248 member radionuclide transport problem used in the convergence test example 1. The second
249 comparison example considers the four-member radionuclide transport problem used in the
250 convergence test example 2. The third comparison example is used to test the accuracy of the computer
251 code for simulating the reactive contaminant transport of a long decay chain. The three comparison
252 examples are executed by comparing the simulated results of the derived analytical solutions with the
253 numerical solutions obtained using the Laplace transformed finite difference (LTFD) technique first
254 developed by Moridis and Reddell (1991). A computer code for the LTFD solution are written in
255 FORTTRAN language with double precision. The details of the FORTRAN computer code is
256 described in Supplement.

257 Figures 2, 3 and 4 depicts the spatial concentration distribution along one longitudinal direction
258 ($y = 50$ m) and two transverse directions ($x = 0$ m and $x = 25$ m) for convergence test example 1
259 at $t = 1,000$ year obtained from analytical solutions and numerical solutions. Figures 5, 6 and 7 present
260 the spatial concentration distribution along one longitudinal direction ($y = 50$ m) and two transverse
261 directions ($x = 0$ m and $x = 25$ m) for the convergence test example 2 at $t = 1,000$ year obtained

262 from analytical solutions and numerical solutions. Excellent agreements between the two solutions for
263 both examples are observed for a wide spectrum of concentration, thus warranting the accuracy and
264 robustness of the developed analytical model.

265 The third example involves a 10 species decay chain previously presented by Srinivasan and
266 Clement (2008a) to evaluate the performance of their one-dimensional analytical solutions. The
267 relevant model parameters are summarized in Tables 8 and 9. Our computer code is also compared
268 against the LTFD solutions for this example. Figure 8 depicts the spatial concentration distribution at
269 $t = 20$ days obtained analytically and numerically. Again there is excellent agreement between the
270 analytical and numerical solutions, demonstrating the performance of our computer code for
271 simulating transport problems with a long decay chain. The three comparison results clearly establish
272 the correctness of the analytical model and the accuracy and capability of the computer code.

273

274 *3.2 Assessing physical and chemical parameters on the radionuclide plume migration*

275 Physical processes and chemical reactions affect the extent of contaminant plumes, as well as
276 concentration levels. To illustrate how the physical processes and chemical reactions affect
277 multispecies plume development, we consider the four-member radionuclide decay chain used in the
278 previous convergence test and solution verification. The model parameters are the same, except that
279 the longitudinal (D_L) and transverse (D_T) dispersion coefficients are varied. Three sets of
280 longitudinal and transverse dispersion coefficients $D_L=1,000$, $D_T=100$; $D_L=1,000$, $D_T=200$;
281 $D_L=2000$, $D_T=200$ (all in $m^2/year$) are tested, all for a simulation time of 1,000 years.

282 Figure 9 illustrates the spatial concentration of four species at $t = 1,000$ year for the three sets of
283 dispersion coefficients. The mobility of plumes of ^{234}U and ^{230}Th is retarded because of their stronger
284 sorption ability. Hence the least retarded ^{226}Ra plume extensively migrated to $200\text{ m} \times 60\text{ m}$ area

285 in the simulation domain, whereas the ^{234}U and ^{230}Th plumes are confined within 60 m × 50 m area
286 in the simulation domain. The moderate mobility of ^{238}Pu reflects the fact that it is a medial sorbed
287 member of this radionuclide decay chain. The high concentration level of ^{234}U accounts for the high
288 first-order decay rate constant of its parent species ^{238}Pu and its own low first-order decay rate constant.
289 The plume extents and concentration levels may be sensitive to longitudinal and transverse dispersion.
290 Increase of the longitudinal and/or transverse dispersion coefficients enhances the spreading of the
291 plume extensively along the longitudinal and/or transverse directions, thereby lowering the plume
292 concentration level. Because the concentration levels of the four radionuclides are influenced by both
293 source release rates and decay chain reactions, ^{230}Th has the least extended plume area, while ^{226}Ra
294 has the greatest plume area for all three set of dispersion coefficients. These dispersion coefficients
295 only affect the size of plumes of the four radionuclide, but the order of their relative plume size remains
296 the same (i.e. $^{226}\text{Ra} > ^{238}\text{Pu} > ^{234}\text{U} > ^{230}\text{Th}$ for the simulated condition). Indeed, in the reactive
297 contaminant transport, the chemical parameters of sorption and decay rate are more important than the
298 physical parameters of dispersion coefficients that govern the order of the plume extents and the
299 concentration levels.

300

301 *3.3 Simulating the natural attenuation of chlorinated solvent plume migration*

302 Natural attenuation is the reduction in concentration and mass of the contaminant due to
303 naturally occurring processes in the subsurface environment. The process is monitored for regulatory
304 purposes to demonstrate continuing attenuation of the contaminant reaching the site-specific
305 regulatory goals within reasonable time, hence, the use of the term monitored natural attenuation
306 (MNA). MNA has been widely accepted as a suitable management option for chlorinated solvent
307 contaminated groundwater. Mathematical model are widely used to evaluate the natural attenuation
308 of plumes at chlorinated solvent sites. The multispecies transport analytical model developed in this

309 study provides an effective tool for evaluating performance of the monitoring natural attenuation of
310 plumes at a chlorinated solvent site because a series of daughter products produced during
311 biodegradation of chlorinated solvent such as $PCE \rightarrow TCE \rightarrow DCE \rightarrow VC \rightarrow ETH$. Thus simulation of
312 the natural attenuation of plumes a chlorinated solvent constitutes an attractive field application
313 example of our multispecies transport model.

314 A study of 45 chlorinated solvent sites by McGuire et al. (2014) found that mathematical
315 models were used at 60% of these sites and that the public domain model BIOCHLOR (Aziz et al.,
316 2000) provided by the Center for Subsurface Modeling Support (CSMoS) of USEPA was the most
317 commonly used model. An illustrated example from BIOCHLOR manual (Aziz et al., 2000) is
318 considered to demonstrate the application of the developed analytical model. This example
319 application demonstrated that BIOCHLOR can reproduce plume movement from 1965 to 1998 at the
320 contaminated site of Cape Canaveral Air Station, Florida. The simulation conditions and transport
321 parameters for this example application are summarized in Table 10. Constant source concentrations
322 rather than exponentially declining source concentration of five-species chlorinated solvents are
323 specified in the $90.7\text{ m} \leq y \leq 122.7\text{ m}$ segment at the inlet boundary ($x = 0$). This means that the
324 exponents (λ_{im}) of Bateman-type sources in Eqs. (16a) or (16b) need to be set to zero for the constant
325 source concentrations and source intensity constants (b_{im}) are set to zero when subscript i does not
326 equal to subscript m . Table 11 lists the coefficients of Bateman-type boundary source used for this
327 example application involving the five-species dissolved chlorinated solvent problem. Spatial
328 concentration contours of five-species at $t = 1$ year obtained from the derived analytical solutions for
329 natural attenuation of chlorinated solvent plumes are depicted in Fig. 10. It is observed that the
330 mobility of plumes is quite sensitive to the species retardation factors, whereas the decay rate
331 constants determine the plume concentration level. The plumes can migrate over a larger region for
332 species having a low retardation factor such as VC. The low decay rate constants such as ETH have

333 higher concentration distribution than the VC. It should be noted that a larger extent of plume
334 observed for ETH in Fig. 10 is mainly attributed the plume mass accumulation from the predecessor
335 species VC that have a larger plume extent. The effect of high retardation of the ETH is hindered by
336 the mass accumulation of the predecessor species VC.

337

338 **4. Conclusions**

339 We present an analytical model with a parsimonious mathematical format for two-dimensional
340 multispecies advective-dispersive transport of decaying contaminants such as radionuclides,
341 chlorinated solvents and nitrogen. The developed model is capable of accounting for the temporal and
342 spatial development of an arbitrary number of sequential first-order decay reactions. The solution
343 procedures involve applying a series of Laplace, finite Fourier cosine and generalized integral
344 transforms to reduce a partial differential equation system to an algebraic system, solving for the
345 algebraic system for each species, and then inversely transforming the concentration of each species
346 in transformed domain into the original domain. Explicit special solutions for Bateman type source
347 problems are derived via the generalized analytical solutions. The convergence of the series expansion
348 of the generalized analytical solution is robust and accurate. These explicit solutions and the computer
349 code are comparing with the results computed by the numerical solutions. The two solutions agree well
350 for a wide spectrum of concentration variations for three test examples. The analytical model is applied
351 to assess the plume development of radionuclide and dissolved chlorinated solvent decay chain. The
352 results show that dispersion only moderately modifies the size of the plumes, without altering the
353 relative order of the plume sizes of different contaminant. It is suggested that retardation coefficients,
354 decay rate constants and the predecessor species plume distribution mainly govern the order of plume
355 size in groundwater. Although there are a number of numerical reactive transport models that can
356 account for multispecies advective-dispersive transport, our analytical model with a computer code

357 that can directly evaluate the two-dimensional temporal-spatial concentration distribution of arbitrary
358 target species without involving the computation of other species. The analytical model developed in
359 this study effectively and accurately predicts the two-dimensional radionuclide and dissolved
360 chlorinated plume migration. It is a useful tool for assessing the ecological and environmental impact
361 of the accidental radionuclide releases such as the Fukushima nuclear disaster where multiple
362 radionuclides leaked through the reactor, subsequently contaminating the local groundwater and ocean
363 seawater in the vicinity of the nuclear plant. It is also a screening model that simulates remediation by
364 natural attenuation of dissolved solvents at chlorinated solvent release sites. **It should be noted the
365 derived analytical model still has its application limitations. The model cannot handle the site with
366 non-uniform groundwater flow or with multiple distinct zones.** Furthermore, the developed model
367 cannot simulate the more complicated decay chain problems such as diverging, converging and
368 branched decay chains. The analytical model for more complicated decay chain problems can be
369 pursued in the near future.

370

371

372

373

374 **Appendix A**

375 **Derivation of analytical solutions**

376 In this appendix, we elaborate on the mathematical procedures for deriving the analytical solutions.

377 The Laplace transforms of Eqs. (7a), (7b), (9)-(12) yield

378
$$\frac{1}{Pe_L} \frac{\partial^2 G_1(X, Y, s)}{\partial X^2} - \frac{\partial G_1(X, Y, s)}{\partial X} + \frac{\rho^2}{Pe_T} \frac{\partial^2 G_1(X, Y, s)}{\partial Y^2} - (R_1 s + \kappa_1) G_1(X, Y, s) = 0 \quad (A1a)$$

379
$$\frac{1}{Pe_L} \frac{\partial^2 G_i(X, Y, s)}{\partial X^2} - \frac{\partial G_i(X, Y, s)}{\partial X} + \frac{\rho^2}{Pe_T} \frac{\partial^2 G_i(X, Y, s)}{\partial Y^2} \quad i = 2, 3, \dots, N \quad (A1b)$$

$$- \kappa_i G_i(X, Y, s) + \kappa_{i-1} G_{i-1}(X, Y, s) = R_i s G_i(X, Y, s)$$

380
$$- \frac{1}{Pe_L} \frac{\partial G_i(X=0, Y, s)}{\partial X} + G_i(X=0, Y, s) = F_i(s) [H(Y - Y_1) - H(Y - Y_2)] \quad 0 \leq Y \leq 1 \quad i = 1 \dots N.$$

381 (A2)

382
$$\frac{\partial G_i(X=1, Y, s)}{\partial X} = 0 \quad 0 \leq Y \leq 1 \quad i = 1 \dots N. \quad (A3)$$

383
$$\frac{\partial G_i(X, Y=0, s)}{\partial Y} = 0 \quad 0 \leq X \leq 1 \quad i = 1 \dots N. \quad (A4)$$

384
$$\frac{\partial G_i(X, Y=1, s)}{\partial Y} = 0 \quad 0 \leq X \leq 1 \quad i = 1 \dots N. \quad (A5)$$

385 where s is the Laplace transform parameter, and $G_i(X, Y, s)$ and $F_i(s)$ are defined by the Laplace

386 transformation relations as

387
$$G_i(X, Y, s) = \int_0^{\infty} e^{-sT} C_i(X, Y, T) dT \quad (A6)$$

388
$$F_i(s) = \int_0^{\infty} e^{-sT} f_i(T) dT \quad (A7)$$

389

390 The finite Fourier cosine transform is used here because it satisfies the transformed governing

391 equations in Eqs. (A1a) and (A2b) and their corresponding boundary conditions in Eqs. (A4) and (A5).

392 Application of the finite Fourier cosine transform on Eqs. (A1)-(A3) leads to

$$393 \quad \frac{1}{Pe_L} \frac{d^2 H_1(X, n, s)}{dX^2} - \frac{dH_1(X, n, s)}{dX} - \left(R_1 s + \kappa_1 + \frac{\rho^2 n^2 \pi^2}{Pe_T} \right) H_1(X, n, s) = 0 \quad (A8a)$$

$$394 \quad \frac{1}{Pe_L} \frac{d^2 H_i(X, n, s)}{dX^2} - \frac{dH_i(X, n, s)}{dX} - \left(R_i s + \kappa_i + \frac{\rho^2 n^2 \pi^2}{Pe_T} \right) H_i(X, n, s) + \kappa_{i-1} H_{i-1}(X, n, s) = 0 \quad (A8b)$$

$$395 \quad -\frac{1}{Pe_L} \frac{dH_i(X=0, n, s)}{dX} + H_i(X=0, n, s) = F_i(s) \Phi(n) \quad (A9)$$

$$396 \quad \frac{dH_i(X=1, n, s)}{dX} = 0 \quad (A10)$$

$$397 \quad \text{where } \Phi(n) = \begin{cases} Y_2 - Y_1 & n = 0 \\ \frac{\sin(n\pi Y_2) - \sin(n\pi Y_1)}{n\pi} & n = 1, 2, 3, \dots \end{cases}, \quad n \text{ is the finite Fourier cosine transform}$$

398 parameter, $H_i(X, n, s)$ is defined by the following conjugate equations (Sneddon, 1972)

$$399 \quad H_i(X, n, s) = \int_0^1 G_i(X, Y, s) \cos(n\pi Y) dY \quad (A11)$$

$$400 \quad G_i(X, Y, s) = H_i(X, n=0, s) + 2 \sum_{n=1}^{n=\infty} H_i(X, n, s) \cos(n\pi Y) \quad (A12)$$

401 Using changes-of-variables, similar to those applied by Chen and Liu (2011), the advective terms

402 in Eqs. (A8a) and A(8b) as well as nonhomogeneous terms in Eq. (A9) can be easily removed. Thus,

403 substitutions of the change-of-variable into Eqs. (A8a), (A8b), (A9) and (A10) result in diffusive-type

404 equations associated with homogeneous boundary conditions

$$405 \quad \frac{1}{Pe_L} \frac{d^2 U_1(X, n, s)}{dX^2} - \left(R_1 s + \kappa_1 + \frac{\rho^2 n^2 \pi^2}{Pe_T} + \frac{Pe_L}{4} \right) U_1(X, n, s) \\ = e^{-\frac{Pe_L}{2} X} \left(R_1 s + \kappa_1 + \frac{\rho^2 n^2 \pi^2}{Pe_T} \right) F_1(s) \Phi(n) \quad (A13a)$$

$$\begin{aligned}
& \frac{1}{Pe_L} \frac{d^2 U_i(X, n, s)}{dX^2} - \left(\frac{Pe_L}{4} + R_1 s + \kappa_1 + \frac{\rho^2 n^2 \pi^2}{Pe_T} \right) U_i(X, n, s) \\
& = e^{-\frac{Pe_L X}{2}} \left(R_1 s + \kappa_1 + \frac{\rho^2 n^2 \pi^2}{Pe_T} \right) F_i(s) \Phi(n) - e^{-\frac{Pe_L X}{2}} \kappa_{i-1} F_{i-1}(s) \Phi(n) - \kappa_{i-1} U_{i-1}(X, n, s)
\end{aligned} \tag{A13b}$$

$$-\frac{dU_i(X=0, n, s)}{dX} + \frac{Pe}{2} U_i(X=0, n, s) = 0 \tag{A14}$$

$$\frac{dU_i(X=1, n, s)}{dX} + \frac{Pe_L}{2} U_i(X=1, n, s) = 0 \tag{A15}$$

where $U_i(X, n, s)$ is defined as the following change-of-variable relation

$$H_i(X, n, s) = F_i(s) \Phi(n) + e^{-\frac{Pe_L X}{2}} U_i(X, n, s) \tag{A16}$$

As detailed in Ozisik (1989), the generalized integral transform pairs for Eqs. (A13a) and (A13b)

and its associated boundary conditions (A14) and (A15) are defined as

$$Z_i(\xi_l, n, s) = \int_0^1 K(\xi_l, X) U_i(X, n, s) dX \tag{A17}$$

$$U_i(X, n, s) = \sum_{l=1}^{\infty} \frac{K(\xi_l, X)}{N(\xi_l)} Z_i(\xi_l, n, s) \tag{A18}$$

where $K(\xi_l, X) = \frac{Pe_L}{2} \sin(\xi_l X) + \xi_l \cos(\xi_l X)$ is the kernel function, $N(\xi_l) = \frac{2}{\frac{Pe_L^2}{4} + Pe_L + \xi_l^2}$,

ξ_l is the eigenvalue, determined from the equation

$$\xi_l \cot \xi_l - \frac{\xi_l^2}{Pe_L} + \frac{Pe_L}{4} = 0 \tag{A19}$$

The generalized integral transforms of Eqs. (13a) and (13b) give

$$-\left(R_1 s + \kappa_1 + \frac{\rho^2 n^2 \pi^2}{Pe_T} + \frac{Pe_L}{4} + \frac{\xi_l^2}{Pe_L} \right) Z_i(\xi_l, n, s) = \left(R_1 s + \kappa_1 + \frac{\rho^2 n^2 \pi^2}{Pe_T} \right) F_1(s) \Phi(n) \Theta(\xi_l) \tag{A20}$$

420
$$-\left(R_i s + \kappa_i + \frac{\rho^2 n^2 \pi^2}{Pe_T} + \frac{Pe_L}{4} + \frac{\xi_l^2}{Pe_L}\right) Z_i(\xi_l, n, s)$$

421
$$= \left(R_i s + \kappa_i + \frac{\rho^2 n^2 \pi^2}{Pe_T}\right) F_i(s) \Phi(n) \Theta(\xi_l) - \kappa_{i-1} F_{i-1}(s) \Phi(n) \Theta(\xi_l) - \kappa_{i-1} Z_{i-1}(\xi_l, n, s)$$

(A21)

421 where
$$\Theta(\xi_l) = \frac{Pe_L \xi_l}{\frac{Pe_L^2}{4} + \xi_l^2}.$$

422 Solving for Eqs. (A20) and (A21) algebraically for each species, $Z_i(\xi_l, n, s)$, in sequence, leads

423 to

424
$$Z_1(\xi_l, n, s) = -\frac{s + \alpha_1 - \beta_1}{s + \alpha_1} F_1(s) \Phi(n) \Theta(\xi_l)$$

(A22)

425
$$Z_2(\xi_l, n, s) = \left[-\frac{s + \alpha_2 - \beta_2}{s + \alpha_2} F_2(s) + \frac{\sigma_2 \beta_1}{(s + \alpha_2)(s + \alpha_1)} F_1(s) \right] \Phi(n) \Theta(\xi_l)$$

(A23)

426
$$Z_3(\xi_l, n, s) = \left[-\frac{s + \alpha_3 - \beta_3}{s + \alpha_3} F_3(s) + \frac{\sigma_3 \beta_2}{(s + \alpha_3)(s + \alpha_2)} F_2(s) \right.$$

(A24)

$$\left. \frac{\sigma_3 \sigma_2 \beta_1}{(s + \alpha_3)(s + \alpha_2)(s + \alpha_1)} F_1(s) \right] \Phi(n) \Theta(\xi_l)$$

427
$$Z_4(\xi_l, n, s) = \left[-\frac{s + \alpha_4 - \beta_4}{s + \alpha_4} F_4(s) + \frac{\sigma_4 \beta_3}{(s + \alpha_4)(s + \alpha_3)} F_3(s) \right.$$

(A25)

$$\left. + \frac{\sigma_4 \sigma_3 \beta_2}{(s + \alpha_4)(s + \alpha_3)(s + \alpha_2)} F_2(s) + \frac{\sigma_4 \sigma_3 \sigma_2 \beta_1}{(s + \alpha_4)(s + \alpha_3)(s + \alpha_2)(s + \alpha_1)} F_1(s) \right] \Phi(n) \Theta(\xi_l)$$

428 where
$$\alpha_i(\xi_l) = \frac{\kappa_i}{R_i} + \frac{\rho^2 n^2 \pi^2}{Pe_T R_i} + \frac{Pe_L}{4 R_i} + \frac{\xi_l^2}{Pe_L R_i}, \quad \beta_i(\xi_l) = \frac{Pe_L}{4 R_i} + \frac{\xi_l^2}{Pe_L R_i}, \quad \sigma_i = \frac{\kappa_{i-1}}{R_i}.$$

429 Upon inspection of Eqs. (A22)-(A25), compact expressions valid for all species can be generalized as

430
$$Z_i(\xi_l, n, s) = [P_i(\xi_l, n, s) + Q_i(\xi_l, n, s)] \Phi(n) \Theta(\xi_l) \quad i = 1, 2, \dots, N$$

(A26)

431 where $P_i(\xi_l, n, s) = -\frac{s + \alpha_i - \beta_i}{s + \alpha_i} F_i(s)$ and $Q_i(\xi_l, n, s) = \sum_{k=0}^{i-2} \frac{\beta_{i-k-1} \prod_{j_1=0}^{j_1=k} \sigma_{i-j_1}}{\prod_{j_2=0}^{j_2=k+1} (s + \alpha_{i-j_2})} F_{i-k-1}(s)$.

432 The solutions in the original domain are obtained by a series of integral transform inversions in
 433 combination with changes-of-variables.

434 The inverse generalized integral transform of Eq. (A26) gives

435
$$W_i(X, n, s) = \sum_{m=1}^{\infty} \frac{K(\xi_l, X)}{N(\xi_l)} [P_i(\xi_l, n, s) + Q_i(\xi_l, n, s)] \Phi(n) \Theta(\xi_l) \quad (\text{A27})$$

436 Using change-of-variable relation of Eq. (A16), one obtains

437
$$H_i(\xi_l, n, s) = F_i(s) \Phi(n) + e^{\frac{Pe_L x_D}{2}} \sum_{m=1}^{\infty} \frac{K(\xi_l, x_D)}{N(\xi_l)} [P_i(\xi_l, n, s) + Q_i(\xi_l, n, s)] \Phi(n) \Theta(\xi_l) \quad (\text{A28})$$

438 The finite Fourier cosine inverse transform of Eq. (A28) results in

439
$$\begin{aligned} G_i(X, Y, s) &= F_i(s) \Phi(n=0) + e^{\frac{Pe_L X}{2}} \cdot \sum_{l=1}^{\infty} \frac{K(\xi_l, X)}{N(\xi_l)} [P_i(\xi_l, n, s) + Q_i(\xi_l, n, s)] \Phi(n=0) \Theta(\xi_l) \\ &+ 2 \sum_{n=1}^{n=\infty} \left\{ F_i(s) \Phi(n) + e^{\frac{Pe_L X}{2}} \sum_{l=1}^{\infty} \frac{K(\xi_l, X)}{N(\xi_l)} [P_i(\xi_l, n, s) + Q_i(\xi_l, n, s)] \Phi(n) \Theta(\xi_l) \right\} \cos(n\pi Y) \end{aligned} \quad (\text{A29})$$

440 The analytical solutions in the original domain will be completed by taking the Laplace inverse
 441 transform of Eq. (A29). $P_i(\xi_l, n, s)$ in Eq. (29) is in the form of the product of two functions . The

442 Laplace transform of $\frac{s + \alpha_i - \beta_i}{s + \alpha_i}$ can be easily obtained as

443
$$L^{-1} \left[\frac{s + \alpha_i - \beta_i}{s + \alpha_i} \right] = \delta(T) - \beta_i e^{-\alpha_i T} \quad (\text{A30})$$

444 Thus, the Laplace inverse of $P_i(\xi_l, n, s)$ can be achieved using the convolution theorem as

445 $p_i(\xi_l, n, T) = L^{-1}[P_i(\xi_l, n, s)] = L^{-1}\left[-\frac{s + \alpha_i - \beta_i}{s + \alpha_i} F_i(s)\right] = -f_i(T) + \beta_i e^{-\alpha_i T} \int_0^T f_i(\tau) e^{\alpha_i \tau} d\tau \quad (\text{A31})$

446 The Laplace inverse of $Q_i(\xi_l, n, s)$ can be also approached using the similar method. By taking

447 Laplace inverse transform on $Q_i(\xi_l, n, s)$, we have

448 $q_i(\xi_l, n, T) = L^{-1}[Q_i(\xi_l, n, s)] = L^{-1}\left[\sum_{k=0}^{i-2} \frac{\beta_{i-k-1} \prod_{j_1=0}^{j_1=k} \sigma_{i-j_1}}{\prod_{j_2=0}^{j_2=k+1} (s + \alpha_{i-j_2})} F_{i-k-1}(s)\right]$

449 $= \sum_{k=0}^{i-2} \beta_{i-k-1} \prod_{j_1=0}^{j_1=k} \sigma_{i-j_1} L^{-1}\left[\frac{1}{\prod_{j_2=0}^{j_2=k+1} (s + \alpha_{i-j_2})} F_{i-k-1}(s)\right] \quad (\text{A32})$

450

451 Expressing $\frac{1}{\prod_{j_2=0}^{j_2=k+1} (s + \alpha_{i-j_2})}$ as the summation of partial fractions and applying the inverse

452 Laplace transform formula, one gets

453 $L^{-1}\left[\frac{1}{\prod_{j_2=0}^{j_2=k+1} (s + \alpha_{i-j_2})}\right] = L^{-1}\left[\sum_{j_2=0}^{j_2=k+1} \frac{1}{\prod_{j_3=i-k-1, j_3 \neq i-j_2}^{j_3=i} (\alpha_{j_3} - \alpha_{i-j_2})(s + \alpha_{i-j_2})}\right]$

454 $= \sum_{j_2=0}^{j_2=k+1} \frac{e^{-\alpha_{i-j_1} T}}{\prod_{j_3=i-k-1, j_3 \neq i-j_1}^{j_3=i} (\alpha_{j_3} - \alpha_{i-j_1})} \quad (\text{A33})$

455

456 Recall that the inverse Laplace transform of $F_{i-k-1}(s)$ is $f_{i-k-1}(T)$. Thus, the Laplace inverse

457 transform of $\frac{1}{\prod_{j_2=0}^{j_2=k+1} (s + \alpha_{i-j_2})} F_{i-k-1}(s)$ in Eq. (1) can be achieved using the convolution integral

458 equation as

$$459 \quad L^{-1} \left[\frac{1}{\prod_{j_2=0}^{j_2=k+1} (s + \alpha_{i-j_2})} F_{i-k-1}(s) \right] = \sum_{j_2=0}^{j_2=k+1} \frac{e^{-\alpha_{i-j_1} T} \int_0^T e^{\alpha_{i-j_1} \tau} f_{i-k-1}(\tau) d\tau}{\prod_{\substack{j_3=i \\ j_3=i-k-1, j_3 \neq i-j_2}} (\alpha_{j_3} - \alpha_{i-j_2})} \quad (A34)$$

460 Putting Eq. (A34) into Eq. (A2) we can obtain the following form:

$$461 \quad q_i(\xi_l, n, T) = \sum_{k=0}^{k=i-2} \beta_{i-k-1} \prod_{j_1=0}^{j_1=k} \sigma_{i-j_1} \sum_{j_2=0}^{j_2=k+1} \frac{e^{-\alpha_{i-j_1} T} \int_0^T e^{\alpha_{i-j_1} \tau} f_{i-k-1}(\tau) d\tau}{\prod_{\substack{j_3=i \\ j_3=i-k-1, j_3 \neq i-j_2}} (\alpha_{j_3} - \alpha_{i-j_2})} \quad (A35)$$

462 Thus, the final solution can be expressed as Eq.(13) with the corresponding functions defined in Eqs.(14)

463 and (15).

464 Note that Eq. (A33) is invalid for some of α_{i-j_2} being identical. For such conditions, we can

465 still reduce $\frac{1}{\prod_{j_2=0}^{j_2=k+1} (s + \alpha_{i-j_2})}$ to a sum of partial fraction expansion. However, it will lead to

466 different Laplace inverse formulae. For example, the following formulae is used for all α_{i-j_2} being

467 identical

$$468 \quad L^{-1} \left[\frac{1}{\prod_{j_2=0}^{j_2=k+1} (s + \alpha_{i-j_2})} \right] = \frac{T^k e^{-\alpha_{i-j_2} T}}{k!} \quad (A36)$$

469 The generalized formulae for the cases with some of α_{i-j_2} being identical will not be provided

470 herein because there are a large number of combinations of α_{i-j_2} . We suggest that the readers can
471 pursue the solutions by following the similar steps for such specific conditions case by case.

472

473 **Acknowledgement**

474 The authors are grateful to the Ministry of Science and Technology, Republic of China, for
475 financial support of this research under contract MOST 103-2221-E-0008-100. The authors thanks
476 three anonymous referees for their helpful comments and suggestions.

477

478 **References**

- 479 Aziz, C. E., Newell, C. J., Gonzales, J. R., Haas P., Clement, T. P., Sun, Y.: BIOCHLOR—Natural
480 attenuation decision support system v1.0, User's Manual, U.S. EPA Report, EPA 600/R-
481 00/008, 2000.
- 482 Barry, D. A., Sposito, G.: Application of the convection-dispersion model to solute transport in finite
483 soil columns, *Soil Sc. Soc. Am. J.*, 52, 3-9, 1988.
- 484 Batu, V.: A generalized two-dimensional analytical solution for hydrodynamic dispersion in bounded
485 media with the first-type boundary condition at the source, *Water Resour. Res.*, 25, 1125-1132,
486 1989.
- 487 Batu, V.: A generalized two-dimensional analytical solute transport model in bounded media for flux-
488 type finite multiple sources, *Water Resour. Res.*, 29, 2881-2892, 1993.
- 489 Batu, V.: A generalized three-dimensional analytical solute transport model for multiple rectangular
490 first-type sources, *J. Hydrol.* 174, 57-82, 1996.
- 491 Bauer, P., Attinger, S., Kinzelbach, W.: Transport of a decay chain in homogeneous porous media:
492 analytical solutions, *J. Contam. Hydrol.* 49, 217-239, 2001.

493 Chen, J. S., Liu, C. W.: Generalized analytical solution for advection-dispersion equation in finite
494 spatial domain with arbitrary time-dependent inlet boundary condition, *Hydrol. Earth Sys. Sci.*,
495 15, 2471-2479, 2011.

496 Chen, J. S., Ni, C. F., Liang, C. P., Chiang, C. C.: Analytical power series solution for contaminant
497 transport with hyperbolic asymptotic distance-dependent dispersivity, *J. Hydrol.*, 362, 142-149,
498 2008a.

499 Chen, J. S., Ni, C. F., Liang, C. P.: Analytical power series solutions to the two-dimensional advection-
500 dispersion equation with distance-dependent dispersivities, *Hydrol. Process.*, 22, 670-678,
501 2008b.

502 Chen, J. S., Chen, J. T., Liu, C. W., Liang, C. P., Lin, C. M.: Analytical solutions to two-dimensional
503 advection–dispersion equation in cylindrical coordinates in finite domain subject to first- and
504 third-type inlet boundary conditions, *J. Hydrol.*, 405, 522-531, 2011.

505 Chen, J. S., Lai, K. H., Liu, C. W., Ni, C. F.: A novel method for analytically solving multi-species
506 advective-dispersive transport equations sequentially coupled with first-order decay reactions.
507 *J. Hydrol.*, 420-421, 191-204, 2012a.

508 Chen, J. S., Liu, C. W., Liang, C. P., Lai, K. H.: Generalized analytical solutions to sequentially
509 coupled multi-species advective-dispersive transport equations in a finite domain subject to an
510 arbitrary time-dependent source boundary condition, *J. Hydrol.*, 456-457, 101-109, 2012b.

511 Cho C. M.: Convective transport of ammonium with nitrification in soil, *Can. J. Soil Sci.*, 51, 339-350,
512 1971.

513 Clement, T. P.: Generalized solution to multispecies transport equations coupled with a first-order
514 reaction-network, *Water Resour. Res.*, 37, 157-163, 2001.

515 Gao, G., Zhan, H., Feng, S., Fu, B., Ma, Y., Huang, G.: A new mobile-immobile model for reactive
516 solute transport with scale-dependent dispersion, *Water Resour. Res.*, 46, W08533
517 doi:10.1029/2009WR008707, 2010.

518 Gao, G., Zhan, H., Feng, S., Huang, G., Fu, B.: A mobile-immobile model with an asymptotic scale-
519 dependent dispersion function, *J. Hydrol.*, 424-425, 172-183, 2012.

520 Gao, G., Fu, B., Zhan, H., Ma, Y.: Contaminant transport in soil with depth-dependent reaction
521 coefficients and time-dependent boundary conditions, *Water Res.*, 47, 2507-2522, 2013.

522 Higashi, K., Pigford, T.: Analytical models for migration of radionuclides in geological sorbing media,
523 *J. Nucl. Sci. Technol.*, 17(10), 700-709, 1980.

524 Leij, F. J., Skaggs, T. H., Van Genuchten, M. Th.: Analytical solution for solute transport in three-
525 dimensional semi-infinite porous media, *Water Resour. Res.*, 27, 2719-2733, 1991.

526 Leij, F. J., Toride, N., van Genuchten, M.Th.: Analytical solutions for non-eq uilibrium solute transport
527 in three-dimensional porous media, *J. Hydrol.*, 151, 193-228, 1993.

528 Lunn, M., Lunn. R.J., Mackay, R.: Determining analytic solution of multiple species contaminant
529 transport with sorption and decay, *J. Hydrol.*, 180, 195-210, 1996.

530 McGuire, T. M., Newell, C. J., Looney, B. B., Vangeas, K. M., Sink, C. H., 2004: Historical analysis
531 of monitored natural attenuation: A survey of 191 chlorinated solvent site and 45 solvent
532 plumes. *Remiat. J.* 15: 99-122.

533 Miele J, Zhan H.: Analytical solutions of one-dimensional multispecies reactive transport in a
534 permeable reactive barrier-aquifer system, *J. Contam. Hydrol.*, 134-135, 54-68, 2012.

535 Montas, H. J.: An analytical solution of the three-component transport equation with application to
536 third-order transport, *Water Resour. Res.*, 39, 1036 doi:10.1029/2002WR00128, 2003.

537 Moridis, G. J., Reddell, D. L.: The Laplace transform finite difference method for simulation of flow
538 through porous media, *Water Resour. Res.*, 27, 1873-1884, 1991.

539 Ozisik, M. N.: *Boundary Value Problems of Heat Conduction*, Dover Publications, Inc., New York,
540 1989.

541 Parlange, J. Y., Starr, J. L., van Genuchten, M. Th., Barry, D. A., Parker, J. C.: Exit condition for
542 miscible displacement experiments in finite columns, *Soil Sci.*, 153, 165-171, 1992.

543 Park, E., Zhan, H.: Analytical solutions of contaminant transport from finite one-, two, three-
544 dimensional sources in a finite-thickness aquifer, *J. Contam. Hydrol.*, 53, 41-61, 2000.

545 Pérez Guerrero, J. S., Skaggs, T. H.: Analytical solution for one-dimensional advection-dispersion
546 transport equation with distance-dependent coefficients, *J. Hydrol.*, 390, 57-65, 2010.

547 Pérez Guerrero, J. S., Pimentel, L. G. G., Skaggs, T. H., van Genuchten, M. Th.: Analytical solution
548 for multi-species contaminant transport subject to sequential first-order decay reactions in finite
549 media, *Transport in Porous Med.*, 80, 357–373, 2009.

550 Pérez Guerrero, J. S., Skaggs, T. H., van Genuchten, M. Th., Analytical solution for multi-species
551 contaminant transport in finite media with time-varying boundary condition, *Transport Porous*
552 *Med.*, 85, 171-188, 2010.

553 Pérez Guerrero, J. S., Pontedeiro, E. M., van Genuchten, M. Th., Skaggs, T. H. : Analytical solutions
554 of the one-dimensional advection–dispersion solute transport equation subject to time-
555 dependent boundary conditions, *Chem. Eng. J.*, 221, 487-491, 2013.

556 Quezada, C. R., Clement, T. P., Lee, K. K.: Generalized solution to multi-dimensional multi-species
557 transport equations coupled with a first-order reaction network involving distinct retardation
558 factors, *Adv. Water Res.*, 27, 507-520, 2004.

559 Sneddon, I. H.: *The Use of Integral Transforms*, McGraw-Hill, New York, 1972.

560 Srinivasan, V., Clement, T. P.: Analytical solutions for sequentially coupled one-dimensional reactive
561 transport problems-Part I: Mathematical derivations, *Adv. Water Resour.*, 31, 203-218, 2008a.

562 Srinivasan, V., Clement, T. P.: Analytical solutions for sequentially coupled one-dimensional reactive

563 transport problems-Part II: Special cases, implementation and testing, *Advances in Water*
564 *Resour.* 31, 219-232, 2008b.

565 Sudicky, E. A., Hwang, H. T., Illman, W. A., Wu, Y. S.: A semi-analytical solution for simulating
566 contaminant transport subject to chain-decay reactions, *J. Contam. Hydrol.*, 144, 20-45, 2013.

567 Sun, Y., Clement, T. P.: A decomposition method for solving coupled multi-species reactive transport
568 problems, *Transport in Porous Med.*, 37, 327-346, 1999.

569 Sun, Y., Peterson, J. N., Clement, T. P.: A new analytical solution for multiple species reactive transport
570 in multiple dimensions, *J. Contam. Hydrol.*, 35, 429-440, [1999a](#).

571 Sun, Y., Petersen, J. N., Clement, T. P., Skeen, R. S.: Development of analytical solutions for multi-
572 species transport with serial and parallel reactions, *Water Resour. Res.*, 35, 185-190, 1999b.

573 van Genuchten, M.Th., Alves, W. J.: Analytical solutions of the one-dimensional convective-dispersive
574 solute transport equation, US Department of Agriculture Technical Bulletin No. 1661, 151pp,
575 1982.

576 van Genuchten, M.Th.: Convective–dispersive transport of solutes involved in sequential first-order
577 decay reactions, *Comput. Geosci.*, 11, 129–147, 1985.

578 Yeh, G.T.: AT123D: Analytical Transient One-, Two-, and Three-Dimensional Simulation of Waste
579 Transport in the Aquifer System. ORNL-5602, Oak Ridge National Laboratory, 1981.

580 Zhan, H., Wen, Z., Gao, G.: An analytical solution of two-dimensional reactive solute transport in an
581 aquifer–aquitard system. *Water Resources Research* 45, W10501. doi:10.1029/2008WR007479,
582 2009.

583 Ziskind, G., Shmueli, H., Gitis, V.: An analytical solution of the convection–dispersion–reaction
584 equation for a finite region with a pulse boundary condition, *Chem. Eng. J.*, 167, 403-408,
585 2011.

586
587

588 **Table 1**

589 Transport parameters used for convergence test example 1 involving the four-species radionuclide
 590 decay chain problem used by van Genuchten (1985)

Parameter	Value
Domain length, L [m]	250
Domain width, W [m]	100
Seepage velocity, v [m year ⁻¹]	100
Longitudinal Dispersion coefficient, D_L [m ² year ⁻¹]	1,000
Transverse Dispersion coefficient, D_T [m ² year ⁻¹]	100
Retardation coefficient, R_i	
^{238}Pu	10,000
^{234}U	14,000
^{230}Th	50,000
^{226}Ra	500
Decay constant, k_i [year ⁻¹]	
^{238}Pu	0.0079
^{234}U	0.0000028
^{230}Th	0.0000087
^{226}Ra	0.00043
Source decay constant, λ_m [year ⁻¹]	
^{238}Pu	0.0089
^{234}U	0.00100280
^{230}Th	0.00100870
^{226}Ra	0.00143

591

592

593 **Table 2**

594 Values for coefficients of Bateman-type boundary source for four-species transport problem used by
 595 van Genuchten (1985)

Species, i	b_{im}			
	$m=1$	$m=2$	$m=3$	$m=4$
$^{238}\text{Pu}, i=1$	1.25			
$^{234}\text{U}, i=2$	-1.25044	1.25044		
$^{230}\text{Th}, i=3$	0.443684×10^{-3}	0.593431	-0.593874	
$^{226}\text{Ra}, i=4$	-0.516740×10^{-6}	0.120853×10^{-1}	-0.122637×10^{-1}	0.178925×10^{-3}

596

597

598 **Table 3**

599 Solution convergence of each species concentration at transect of inlet boundary ($x = 0$) for four-
 600 species radionuclide transport problem considering simulated domain of $L = 250$ m, $W = 100$ m,
 601 subject to Bateman-type sources located at $40 \text{ m} \leq y \leq 60 \text{ m}$ for $t = 1,000$ year ($M =$ number of
 602 terms summed for inverse generalized integral transform; $N =$ number of terms summed for inverse
 603 finite Fourier cosine transform). When we investigate the required M for inverse generalized integral
 604 transform, $N=16,000$ for the finite Fourier cosine transform inverse are used. When we investigate the
 605 required N for inverse finite Fourier cosine transform, $M=1,600$ for the generalized transform inverse
 606 are used.

607



x [m]	y [m]	$M = 100$	$M = 200$	$M = 400$	$M = 800$	$M = 1,600$
0	30	2.714E-07	2.712E-07	2.711E-07	2.710E-07	2.710E-07
0	34	3.412E-06	3.412E-06	3.411E-06	3.411E-06	3.411E-06
0	38	2.677E-05	2.677E-05	2.677E-05	2.677E-05	2.677E-05
0	46	1.608E-04	1.609E-04	1.609E-04	1.609E-04	1.609E-04
0	50	1.637E-04	1.637E-04	1.637E-04	1.637E-04	1.637E-04
x [m]	y [m]	$N = 1,000$	$N = 2,000$	$N = 4,000$	$N = 8,000$	$N = 16,000$
0	30	2.723E-07	2.713E-07	2.711E-07	2.710E-07	2.710E-07
0	34	3.413E-06	3.412E-06	3.411E-06	3.411E-06	3.411E-06
0	38	2.677E-05	2.677E-05	2.677E-05	2.677E-05	2.677E-05
0	46	1.609E-04	1.609E-04	1.609E-04	1.609E-04	1.609E-04
0	50	1.637E-04	1.637E-04	1.637E-04	1.637E-04	1.637E-04

608



x [m]	y [m]	$M = 25$	$M = 50$	$M = 100$	$M = 200$	$M = 400$
0	32	1.092E-03	1.091E-03	1.090E-03	1.090E-03	1.090E-03
0	34	4.829E-03	4.827E-03	4.826E-03	4.826E-03	4.825E-03
0	38	5.745E-02	5.753E-02	5.753E-02	5.753E-02	5.753E-02
0	46	3.999E-01	4.004E-01	4.005E-01	4.005E-01	4.005E-01
0	50	4.044E-01	4.049E-01	4.049E-01	4.049E-01	4.049E-01
x [m]	y [m]	$N = 500$	$N = 1,000$	$N = 2,000$	$N = 4,000$	$N = 8,000$
0	32	1.107E-03	1.094E-03	1.091E-03	1.090E-03	1.090E-03
0	34	4.850E-03	4.831E-03	4.827E-03	4.826E-03	4.825E-03
0	38	5.761E-02	5.755E-02	5.753E-02	5.753E-02	5.752E-02

0	46	4.0005E-01	4.005E-01	4.005E-01	4.005E-01	4.005E-01
0	50	4.049E-01	4.049E-01	4.049E-01	4.049E-01	4.049E-01

609

^{230}Th

x [m]	y [m]	$M = 100$	$M = 200$	$M = 400$	$M = 800$	$M = 1,600$
0	34	1.498E-06	1.495E-06	1.493E-06	1.492E-06	1.492E-06
0	38	4.269E-05	4.267E-05	4.267E-05	4.266E-05	4.266E-05
0	42	6.847E-04	6.848E-04	6.848E-04	6.848E-04	6.848E-04
0	46	7.259E-04	7.260E-04	7.260E-04	7.260E-04	7.260E-04
0	50	7.273E-04	7.274E-04	7.274E-04	7.274E-04	7.274E-04
x [m]	y [m]	$N = 1,000$	$N = 2,000$	$N = 4,000$	$N = 8,000$	$N = 16,000$
0	34	1.514E-06	1.497E-06	1.493E-06	1.492E-06	1.492E-06
0	38	4.274E-05	4.268E-05	4.267E-05	4.266E-05	4.266E-05
0	42	6.847E-04	6.848E-04	6.848E-04	6.848E-04	6.848E-04
0	46	7.259E-04	7.260E-04	7.260E-04	7.260E-04	7.260E-04
0	50	7.274E-04	7.274E-04	7.274E-04	7.274E-04	7.274E-04

610

^{226}Ra

x [m]	y [m]	$M = 50$	$M = 100$	$M = 200$	$M = 400$	$M = 800$
0	18	3.084E-08	3.082E-08	3.082E-08	3.081E-08	3.081E-08
0	24	1.294E-07	1.293E-07	1.293E-07	1.293E-07	1.293E-07
0	28	3.492E-07	3.492E-07	3.492E-07	3.492E-07	3.492E-07
0	44	2.217E-05	2.222E-05	2.223E-05	2.223E-05	2.223E-05
0	50	2.425E-05	2.430E-05	2.431E-05	2.431E-05	2.431E-05
x [m]	y [m]	$N = 1,000$	$N = 2,000$	$N = 4,000$	$N = 8,000$	$N = 16,000$
0	18	3.086E-08	3.082E-08	3.082E-08	3.081E-08	3.081E-08
0	24	1.294E-07	1.293E-07	1.293E-07	1.293E-07	1.293E-07
0	28	3.493E-07	3.492E-07	3.492E-07	3.492E-07	3.492E-07
0	44	2.223E-05	2.223E-05	2.223E-05	2.223E-05	2.223E-05
0	50	2.431E-05	2.431E-05	2.431E-05	2.431E-05	2.431E-05

611

612

613

614 **Table 4**

615 Solution convergence of each species concentration at transect of $x = 25$ m for four-species
 616 radionuclide transport problem considering simulated domain of $L = 250$ m, $W = 100$ m, subject
 617 to Bateman-type sources located at $40\text{ m} \leq y \leq 60\text{ m}$ for $t = 1,000$ year ($M =$ number of terms
 618 summed for inverse generalized integral transform; $N =$ number of terms summed for inverse finite
 619 Fourier cosine transform). When we investigate the required M for inverse generalized integral
 620 transform, $N=160$ for the finite Fourier cosine transform inverse are used. When we investigate the
 621 required N for inverse finite Fourier cosine transform, $M=1,600$ for the generalized transform inverse
 622 are used.

623



x [m]	y [m]	$M = 100$	$M = 200$	$M = 400$	$M = 800$	$M = 1,600$
25	28	5.531E-08	5.576E-08	5.580E-08	5.580E-08	5.580E-08
25	30	2.319E-07	2.312E-07	2.312E-07	2.311E-07	2.311E-07
25	38	1.106E-05	1.106E-05	1.106E-05	1.106E-05	1.106E-05
25	46	3.430E-05	3.430E-05	3.430E-05	3.430E-05	3.430E-05
25	50	3.616E-05	3.616E-05	3.616E-05	3.616E-05	3.616E-05
x [m]	y [m]	$N = 10$	$N = 20$	$N = 40$	$N = 80$	$N = 160$
25	28	-7.841E-07	9.961E-08	5.579E-08	5.580E-08	5.580E-08
25	30	-4.063E-07	2.616E-07	2.312E-07	2.311E-07	2.311E-07
25	38	1.195E-05	1.114E-05	1.106E-05	1.106E-05	1.106E-05
25	46	3.404E-05	3.441E-05	3.430E-05	3.430E-05	3.430E-05
25	50	3.817E-05	3.606E-05	3.616E-05	3.616E-05	3.616E-05

624



x [m]	y [m]	$M = 100$	$M = 200$	$M = 400$	$M = 800$	$M = 1,600$
25	30	9.734E-05	9.612E-05	9.594E-05	9.592E-05	9.592E-05
25	34	1.727E-03	1.725E-03	1.724E-03	1.724E-03	1.724E-03
25	38	1.167E-02	1.167E-02	1.167E-02	1.167E-02	1.167E-02
25	46	4.023E-02	4.024E-02	4.024E-02	4.024E-02	4.024E-02
25	50	4.177E-02	4.178E-02	4.178E-02	4.178E-02	4.178E-02
x [m]	y [m]	$N = 10$	$N = 20$	$N = 40$	$N = 80$	$N = 160$
25	30	-9.427E-04	1.728E-04	9.610E-05	9.592E-05	9.592E-05
25	34	3.154E-03	1.588E-03	1.725E-03	1.724E-03	1.724E-03
25	38	1.324E-02	1.186E-02	1.167E-02	1.167E-02	1.167E-02

25	46	3.984E-02	4.049E-02	4.024E-02	4.024E-02	4.024E-02
25	50	4.487E-02	4.153E-02	4.178E-02	4.178E-02	4.178E-02

625

626

 ^{230}Th

x [m]	y [m]	$M = 100$	$M = 200$	$M = 400$	$M = 800$	$M = 1,600$
25	30	1.822E-08	1.379E-08	1.312E-08	1.305E-08	1.305E-08
25	34	3.288E-07	3.207E-07	3.195E-07	3.193E-07	3.193E-07
25	38	2.766E-06	2.740E-06	2.735E-06	2.735E-06	2.735E-06
25	46	1.013E-05	1.015E-05	1.015E-05	1.015E-05	1.015E-05
25	50	1.043E-05	1.045E-05	1.045E-05	1.045E-05	1.045E-05
x [m]	y [m]	$N = 10$	$N = 20$	$N = 40$	$N = 80$	$N = 160$
25	30	-2.948E-07	4.484E-08	1.320E-08	1.305E-08	1.305E-08
25	34	7.000E-07	2.632E-07	3.196E-07	3.193E-07	3.193E-07
25	38	3.246E-06	2.816E-06	2.735E-06	2.735E-06	2.735E-06
25	46	1.005E-05	1.025E-05	1.015E-05	1.015E-05	1.015E-05
25	50	1.134E-05	1.035E-05	1.045E-05	1.045E-05	1.045E-05

627

 ^{226}Ra

x [m]	y [m]	$M = 25$	$M = 50$	$M = 100$	$M = 200$	$M = 400$
25	10	2.681E-08	2.757E-08	2.767E-08	2.765E-08	2.765E-08
25	14	6.580E-08	6.665E-08	6.676E-08	6.674E-08	6.674E-08
25	18	1.606E-07	1.615E-07	1.617E-07	1.617E-07	1.617E-07
25	42	1.686E-05	1.658E-05	1.656E-05	1.656E-05	1.656E-05
25	50	2.315E-05	2.278E-05	2.277E-05	2.277E-05	2.277E-05
x [m]	y [m]	$N = 10$	$N = 20$	$N = 40$	$N = 80$	$N = 160$
25	10	-5.355E-08	3.027E-08	2.766E-08	2.765E-08	2.765E-08
25	14	7.068E-08	6.392E-08	6.675E-08	6.674E-08	6.674E-08
25	18	2.642E-07	1.640E-07	1.617E-07	1.617E-07	1.617E-07
25	42	1.624E-05	1.655E-05	1.656E-05	1.656E-05	1.656E-05
25	50	2.311E-05	2.275E-05	2.277E-05	2.277E-05	2.277E-05

628

629

630 **Table 5**

631 Solution convergence of each species concentration at transect of exit boundary ($x = 250$ m) for four-
 632 species radionuclide transport problem considering simulated domain of $L = 250$ m, $W = 100$ m
 633 subject to Bateman-type sources located at $40\text{ m} \leq y \leq 60\text{ m}$ for $t = 1000$ year ($M =$ number of
 634 terms summed for inverse generalized integral transform and $N =$ number of terms summed for
 635 inverse finite Fourier cosine transform). When we investigate the required M for inverse generalized
 636 integral transform, $N=16$ for the finite Fourier cosine transform inverse are used. When we investigate
 637 the required N for inverse finite Fourier cosine transform, $M=6,400$ for the generalized transform
 638 inverse are used.

639

640

^{226}Ra

x [m]	y [m]	$M = 400$	$M = 800$	$M = 1,600$	$M = 3,200$	$M = 6,400$
250	2	2.289E-08	1.842E-08	1.814E-08	1.812E-08	1.812E-08
250	14	5.617E-08	5.060E-08	5.025E-08	5.022E-08	5.022E-08
250	26	1.528E-07	1.420E-07	1.413E-07	1.413E-07	1.413E-07
250	38	3.757E-07	2.743E-07	2.678E-07	2.674E-07	2.674E-07
250	50	1.645E-07	3.208E-07	3.306E-07	3.312E-07	3.312E-07
x [m]	y [m]	$N = 1$	$N = 2$	$N = 4$	$N = 8$	$N = 16$
250	2	1.529E-07	-1.848E-09	1.892E-08	1.812E-08	1.812E-08
250	14	1.529E-07	5.348E-08	4.946E-08	5.022E-08	5.022E-08
250	26	1.529E-07	1.627E-07	1.414E-07	1.413E-07	1.413E-07
250	38	1.529E-07	2.666E-07	2.680E-07	2.674E-07	2.674E-07
250	50	1.529E-07	3.089E-07	3.303E-07	3.312E-07	3.312E-07

641

642

643 **Table 6**

644 Solution convergence of each species concentration at transect of inlet boundary ($x = 0$ m) for four-
 645 species radionuclide transport problem considering simulated domain of $L = 2,500$ m, $W = 100$ m
 646 subject to Bateman-type sources located at $45 \text{ m} \leq y \leq 55 \text{ m}$ for $t = 1,000$ year ($M =$ number of
 647 terms summed for inverse generalized integral transform; $N =$ number of terms summed for inverse
 648 finite Fourier cosine transform). When we investigate the required M for inverse generalized integral
 649 transform, $N=12,800$ for the finite Fourier cosine transform inverse are used. When we investigate the
 650 required N for inverse finite Fourier cosine transform, $M=6,400$ for the generalized transform inverse
 651 are used.

652

653



x [m]	y [m]	$M = 400$	$M = 800$	$M = 1,600$	$M = 3,200$	$M = 6,400$
0	36	5.395E-07	5.391E-07	5.389E-07	5.387E-07	5.387E-07
0	38	1.908E-06	1.908E-06	1.908E-06	1.907E-06	1.907E-06
0	42	1.640E-05	1.642E-05	1.642E-05	1.642E-05	1.642E-05
0	46	1.203E-04	1.199E-04	1.198E-04	1.198E-04	1.198E-04
0	50	1.522E-04	1.524E-04	1.525E-04	1.525E-04	1.525E-04
x [m]	y [m]	$N = 2,000$	$N = 4,000$	$N = 8,000$	$N = 16,000$	$N = 32,000$
0	36	5.392E-07	5.389E-07	5.388E-07	5.387E-07	5.387E-07
0	38	1.908E-06	1.908E-06	1.907E-06	1.907E-06	1.907E-06
0	42	1.642E-05	1.642E-05	1.642E-05	1.642E-05	1.642E-05
0	46	1.198E-04	1.198E-04	1.198E-04	1.198E-04	1.199E-04
0	50	1.525E-04	1.525E-04	1.525E-04	1.525E-04	1.525E-04

654



x [m]	y [m]	$M = 800$	$M = 1,600$	$M = 3,200$	$M = 6,400$	$M = 12,800$
0	36	4.817E-04	4.815E-04	4.815E-04	4.814E-04	4.814E-04
0	38	2.348E-03	2.348E-03	2.348E-03	2.348E-03	2.348E-03
0	44	1.011E-01	1.012E-01	1.012E-01	1.012E-01	1.012E-01
0	48	3.704E-01	3.705E-01	3.705E-01	3.705E-01	3.705E-01
0	50	3.862E-01	3.864E-01	3.864E-01	3.864E-01	3.864E-01
x [m]	y [m]	$N = 4,000$	$N = 8,000$	$N = 16,000$	$N = 32,000$	$N = 64,000$
0	36	4.818E-04	4.816E-04	4.815E-04	4.814E-04	4.814E-04
0	38	2.348E-03	2.348E-03	2.348E-03	2.348E-03	2.348E-03

0	44	1.013E-01	1.013E-01	1.012E-01	1.012E-01	1.012E-01
0	48	3.705E-01	3.705E-01	3.705E-01	3.705E-01	3.705E-01
0	50	3.864E-01	3.864E-01	3.864E-01	3.864E-01	3.864E-01

655

^{230}Th

x [m]	y [m]	$M = 400$	$M = 800$	$M = 1,600$	$M = 3,200$	$M = 6,400$
0	40	3.429E-06	3.427E-06	3.424E-06	3.423E-06	3.423E-06
0	42	1.773E-05	1.783E-05	1.782E-05	1.782E-05	1.782E-05
0	44	1.028E-04	1.089E-04	1.093E-04	1.093E-04	1.093E-04
0	48	7.095E-04	7.089E-04	7.090E-04	7.090E-04	7.090E-04
0	50	7.210E-04	7.205E-04	7.206E-04	7.206E-04	7.206E-04
x [m]	y [m]	$N = 2,000$	$N = 4,000$	$N = 8,000$	$N = 16,000$	$N = 32,000$
0	40	3.430E-06	3.425E-06	3.424E-06	3.423E-06	3.423E-06
0	42	1.783E-05	1.782E-05	1.782E-05	1.782E-05	1.782E-05
0	44	1.093E-04	1.093E-04	1.093E-04	1.093E-04	1.093E-04
0	48	7.090E-04	7.090E-04	7.090E-04	7.090E-04	7.090E-04
0	50	7.206E-04	7.206E-04	7.206E-04	7.206E-04	7.206E-04

656

^{226}Ra

x [m]	y [m]	$M = 400$	$M = 800$	$M = 1,600$	$M = 3,200$	$M = 6,400$
0	24	3.557E-08	3.556E-08	3.556E-08	3.555E-08	3.555E-08
0	28	9.276E-08	9.274E-08	9.273E-08	9.273E-08	9.273E-08
0	40	2.159E-06	2.159E-06	2.159E-06	2.159E-06	2.159E-06
0	44	7.739E-06	7.809E-06	7.813E-06	7.813E-06	7.813E-06
0	50	2.072E-05	2.082E-05	2.083E-05	2.084E-05	2.084E-05
x [m]	y [m]	$N = 1,000$	$N = 2,000$	$N = 4,000$	$N = 8,000$	$N = 16,000$
0	24	3.559E-08	3.557E-08	3.556E-08	3.555E-08	3.555E-08
0	28	9.278E-08	9.275E-08	9.274E-08	9.273E-08	9.273E-08
0	40	2.159E-06	2.159E-06	2.159E-06	2.159E-06	2.159E-06
0	44	7.815E-06	7.814E-06	7.813E-06	7.813E-06	7.813E-06
0	50	2.084E-05	2.084E-05	2.084E-05	2.084E-05	2.084E-05

657

658

659 **Table 7**

660 Solution convergence of each species concentration at transect of $x = 250$ m for four-species
 661 radionuclide transport problem considering simulated domain of $L = 2,500$ m, $W = 100$ m subject
 662 to Bateman-type sources located at $45 \text{ m} \leq y \leq 55 \text{ m}$ for $t = 1,000$ year ($M =$ number of terms
 663 summed for inverse generalized integral transform; $N =$ number of terms summed for inverse finite
 664 Fourier cosine transform). When we investigate the required M for inverse generalized integral
 665 transform, $N=160$ for the finite Fourier cosine transform inverse are used. When we investigate the
 666 required N for inverse finite Fourier cosine transform, $M=12,800$ for the generalized transform inverse
 667 are used.

668

 ^{238}Pu

x [m]	y [m]	$M = 200$	$M = 400$	$M = 800$	$M = 1,600$	$M = 3,200$
25	32	2.578E-08	2.569E-08	2.564E-08	2.563E-08	2.563E-08
25	34	1.153E-07	1.162E-07	1.161E-07	1.161E-07	1.161E-07
25	40	3.485E-06	3.661E-06	3.661E-06	3.661E-06	3.661E-06
25	46	2.262E-05	2.176E-05	2.163E-05	2.163E-05	2.163E-05
25	50	2.752E-05	2.920E-05	2.929E-05	2.929E-05	2.929E-05
x [m]	y [m]	$N = 10$	$N = 20$	$N = 40$	$N = 80$	$N = 160$
25	32	-7.217E-07	4.318E-08	2.558E-08	2.563E-08	2.563E-08
25	34	-1.422E-06	1.470E-07	1.162E-07	1.161E-07	1.161E-07
25	40	4.741E-06	3.665E-06	3.661E-06	3.661E-06	3.661E-06
25	46	2.175E-05	2.155E-05	2.163E-05	2.163E-05	2.163E-05
25	50	2.713E-05	2.938E-05	2.929E-05	2.929E-05	2.929E-05

669

 ^{234}U

x [m]	y [m]	$M = 200$	$M = 400$	$M = 800$	$M = 1,600$	$M = 3,200$
25	34	3.937E-05	4.038E-05	4.022E-05	4.019E-05	4.019E-05
25	36	2.029E-04	2.162E-04	2.160E-04	2.159E-04	2.159E-04
25	42	5.649E-03	7.897E-03	7.936E-03	7.936E-03	7.936E-03
25	46	2.695E-02	2.593E-02	2.565E-02	2.564E-02	2.564E-02
25	50	2.913E-02	3.552E-02	3.585E-02	3.586E-02	3.586E-02
x [m]	y [m]	$N = 10$	$N = 20$	$N = 40$	$N = 80$	$N = 160$
25	34	-2.184E-03	1.134E-04	4.038E-05	4.019E-05	4.019E-05
25	36	-2.113E-03	1.975E-04	2.158E-04	2.159E-04	2.159E-04

25	42	1.118E-02	8.092E-03	7.936E-03	7.936E-03	7.936E-03
25	46	2.580E-02	2.544E-02	2.564E-02	2.564E-02	2.564E-02
25	50	3.262E-02	3.608E-02	3.586E-02	3.586E-02	3.586E-02

670

671

^{230}Th

x [m]	y [m]	$M = 800$	$M = 1,600$	$M = 3,200$	$M = 6,400$	$M = 12,800$
25	36	3.192E-08	3.181E-08	3.180E-08	3.179E-08	3.179E-08
25	38	1.578E-07	1.576E-07	1.576E-07	1.576E-07	1.576E-07
25	44	3.838E-06	3.914E-06	3.914E-06	3.914E-06	3.914E-06
25	48	8.531E-06	8.539E-06	8.539E-06	8.539E-06	8.539E-06
25	50	9.253E-06	9.261E-06	9.261E-06	9.262E-06	9.262E-06
x [m]	y [m]	$N = 10$	$N = 20$	$N = 40$	$N = 80$	$N = 160$
25	36	-6.448E-07	2.862E-08	3.167E-08	3.179E-08	3.179E-08
25	38	-1.271E-07	1.141E-07	1.577E-07	1.576E-07	1.576E-07
25	44	4.705E-06	3.925E-06	3.914E-06	3.914E-06	3.914E-06
25	48	7.869E-06	8.534E-06	8.540E-06	8.539E-06	8.539E-06
25	50	8.345E-06	9.353E-06	9.261E-06	9.262E-06	9.262E-06

672

^{226}Ra

x [m]	y [m]	$M = 100$	$M = 200$	$M = 400$	$M = 800$	$M = 1600$
25	12	1.268E-08	1.273E-08	1.272E-08	1.272E-08	1.272E-08
25	18	4.817E-08	4.822E-08	4.821E-08	4.821E-08	4.821E-08
25	26	2.830E-07	2.824E-07	2.824E-07	2.824E-07	2.824E-07
25	42	8.794E-06	7.484E-06	7.578E-06	7.579E-06	7.579E-06
25	50	1.761E-05	1.449E-05	1.494E-05	1.497E-05	1.497E-05
x [m]	y [m]	$N = 10$	$N = 20$	$N = 40$	$N = 80$	$N = 160$
25	12	8.791E-08	1.264E-08	1.272E-08	1.272E-08	1.272E-08
25	18	-1.512E-07	4.713E-08	4.821E-08	4.821E-08	4.821E-08
25	26	5.221E-07	2.830E-07	2.824E-07	2.824E-07	2.824E-07
25	42	7.960E-06	7.587E-06	7.578E-06	7.579E-06	7.579E-06
25	50	1.458E-05	1.498E-05	1.494E-05	1.497E-05	1.497E-05

673

675 **Table 8**
676 Transport parameters used for verification example 2 involving the ten-species transport problem
677 used by Srinivasan and Clement (2008b)

Parameter	Value
Domain length, L [m]	250
Domain width, W [m]	100
Seepage velocity, v [m year ⁻¹]	5
Longitudinal Dispersion coefficient, D_L [m ² year ⁻¹]	50
Transverse Dispersion coefficient, D_T [m ² year ⁻¹]	50
Retardation coefficient, R_i $i=1, 2, \dots, 10$	1.9, 1, 1.4, 1, 5, 8, 1.4, 3.1, 1, 1
Decay constant, k_i [year ⁻¹] $i=1, 2, \dots, 10$	3, 2, 1.5, 1.25, 2.75, 1, 0.75, 0.5, 0.25, 0.1
Source decay constant, λ_m [year ⁻¹] $m=1, 2, \dots, 10$	0.1, 0.75, 0.5, 0.25, 0, 0, 0.3, 1, 0, 0.65

678

679

680

681

682 **Table 9**

683 Coefficients of Bateman-type boundary source for ten-species transport problem used by Srinivasan
684 and Clement (2008b)

Species, i	b_{im}									
	$m=1$	$m=2$	$m=3$	$m=4$	$m=5$	$m=6$	$m=7$	$m=8$	$m=9$	$m=10$
Species 1	10									
Species 2	0	5								
Species 3	0	0	2.5							
Species 4	0	0	0	0						
Species 5	0	0	0	0	10					
Species 6	0	0	0	0	0	5				
Species 7	0	0	0	0	0	0	2.5			
Species 8	0	0	0	0	0	0	0	0		
Species 9	0	0	0	0	0	0	0	0	0	
Species 10	0	0	0	0	0	0	0	0	0	0

685

686

687

688

689

690 **Table 10**

691 Transport parameters used for example application involving the five-species dissolved chlorinated
 692 solvent problem used by BIOCHLOR.

Parameter	Value
Domain length, L [m]	330.7
Domain width, W [m]	213.4
Seepage velocity, v [m year ⁻¹]	34.0
Longitudinal dispersion coefficient, D_L [m ² year ⁻¹]	449
Transverse dispersion coefficient, D_T [m ² year ⁻¹]	44.9
Retardation coefficient, R_i [-]	
<i>PCE</i>	7.13
<i>TCE</i>	2.87
<i>DCE</i>	2.8
<i>VC</i>	1.43
<i>ETH</i>	5.35
Decay constant, k_i [year ⁻¹]	
<i>PCE</i>	2
<i>TCE</i>	1
<i>DCE</i>	0.7
<i>VC</i>	0.4
<i>ETH</i>	0
Source decay rate constant, λ_m [year ⁻¹]	
<i>PCE</i>	0
<i>TCE</i>	0
<i>DCE</i>	0
<i>VC</i>	0
<i>ETH</i>	0

693 **Table 11**

694 Coefficients of Bateman-type boundary source used for example application involving the five-
695 species dissolved chlorinated solvent problem used by BIOCHLOR.

Species, i	b_{im}				
	$m=1$	$m=2$	$m=3$	$m=4$	$m=5$
$PCE, i=1$	0.056				
$TCE, i=2$		15.8			
$DCE, i=3$			98.5		
$VC, i=4$				3.08	
$ETH, i=5$					0.03

696

697

698

699

700

701

702

703

704 **Figures Captions**

705 Fig. 1. Schematic representation of two-dimensional transport of decaying contaminants in a uniform
706 flow field with flux boundary source located at of the inlet boundary.

707 Fig. 2. Comparison of spatial concentration profiles of four species along the longitudinal direction
708 (=50 m) at $t = 1,000$ years obtained from derived analytical solutions and numerical
709 solutions for convergence test example 1 of four-member radionuclide decay chain

710 $^{238}\text{Pu} \rightarrow ^{234}\text{U} \rightarrow ^{230}\text{Th} \rightarrow ^{226}\text{Ra}$.

711 Fig. 3. Comparison of spatial concentration profiles of four species along the transverse direction (=0
712 m) at $t = 1,000$ years obtained from derived analytical solutions and numerical solutions
713 for convergence test example 1 of four-member radionuclide decay chain

714 $^{238}\text{Pu} \rightarrow ^{234}\text{U} \rightarrow ^{230}\text{Th} \rightarrow ^{226}\text{Ra}$.

715 Fig. 4. Comparison of spatial concentration profiles of four species along the transverse direction
716 (=25 m) at $t = 1,000$ years obtained from derived analytical solutions and numerical
717 solutions for convergence test example 1 of four-member radionuclide decay chain

718 $^{238}\text{Pu} \rightarrow ^{234}\text{U} \rightarrow ^{230}\text{Th} \rightarrow ^{226}\text{Ra}$.

719 Fig. 5. Comparison of spatial concentration profiles of four species along the longitudinal direction
720 (=50 m) at $t = 1,000$ years obtained from derived analytical solutions and numerical
721 solutions for convergence test example 2 of four-member radionuclide decay chain

722 $^{238}\text{Pu} \rightarrow ^{234}\text{U} \rightarrow ^{230}\text{Th} \rightarrow ^{226}\text{Ra}$.

723 Fig. 6. Comparison of spatial concentration profiles of four species along the transverse direction (=0

724 m) at $t = 1,000$ years obtained from derived analytical solutions and numerical solutions
725 for convergence test example 2 of four-member radionuclide decay chain
726 $^{238}\text{Pu} \rightarrow ^{234}\text{U} \rightarrow ^{230}\text{Th} \rightarrow ^{226}\text{Ra}$.

727 Fig. 7. Comparison of spatial concentration profiles of four species along the transverse direction
728 ($=25$ m) at $t = 1,000$ years obtained from derived analytical solutions and numerical
729 solutions for convergence test example 2 of four-member radionuclide decay chain
730 $^{238}\text{Pu} \rightarrow ^{234}\text{U} \rightarrow ^{230}\text{Th} \rightarrow ^{226}\text{Ra}$.

731 Fig. 8. Comparison of spatial concentration profiles of ten-species along x -direction at $t = 20$ days
732 obtained from derived analytical solutions and numerical solutions for the test example 3
733 of ten species decay chain used by Srinivasan and Clement (2008b).

734 Fig. 9. Effects of physical processes and chemical reactions on the concentration contours of four-
735 species at $t = 1,000$ years obtained from derived analytical solutions for four-member decay
736 chain $^{238}\text{Pu} \rightarrow ^{234}\text{U} \rightarrow ^{230}\text{Th} \rightarrow ^{226}\text{Ra}$.

737 Fig. 10. Spatial concentration contours of five-species at $t = 1$ year obtained from derived analytical
738 solutions for natural attenuation of chlorinated solvent plumes $\text{PCE} \rightarrow \text{TCE} \rightarrow \text{DCE} \rightarrow \text{VC}$
739 $\rightarrow \text{ETH}$.

740

741

742

743

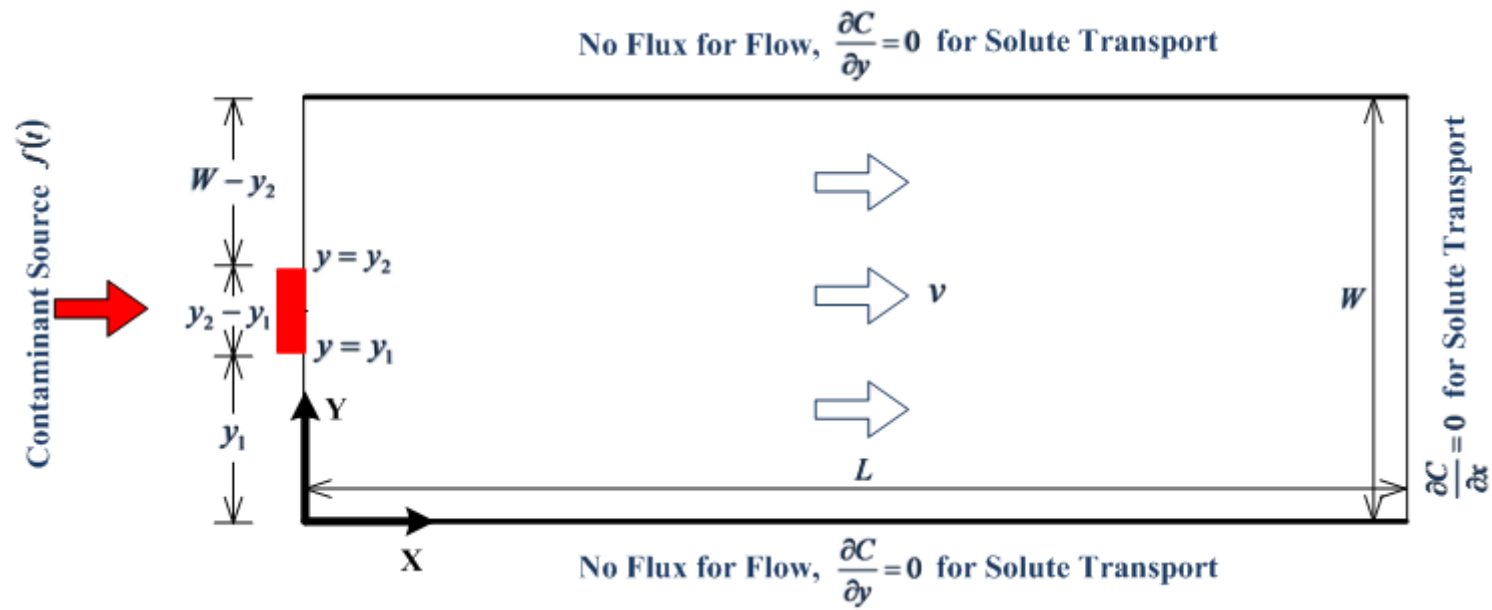


Fig. 1.

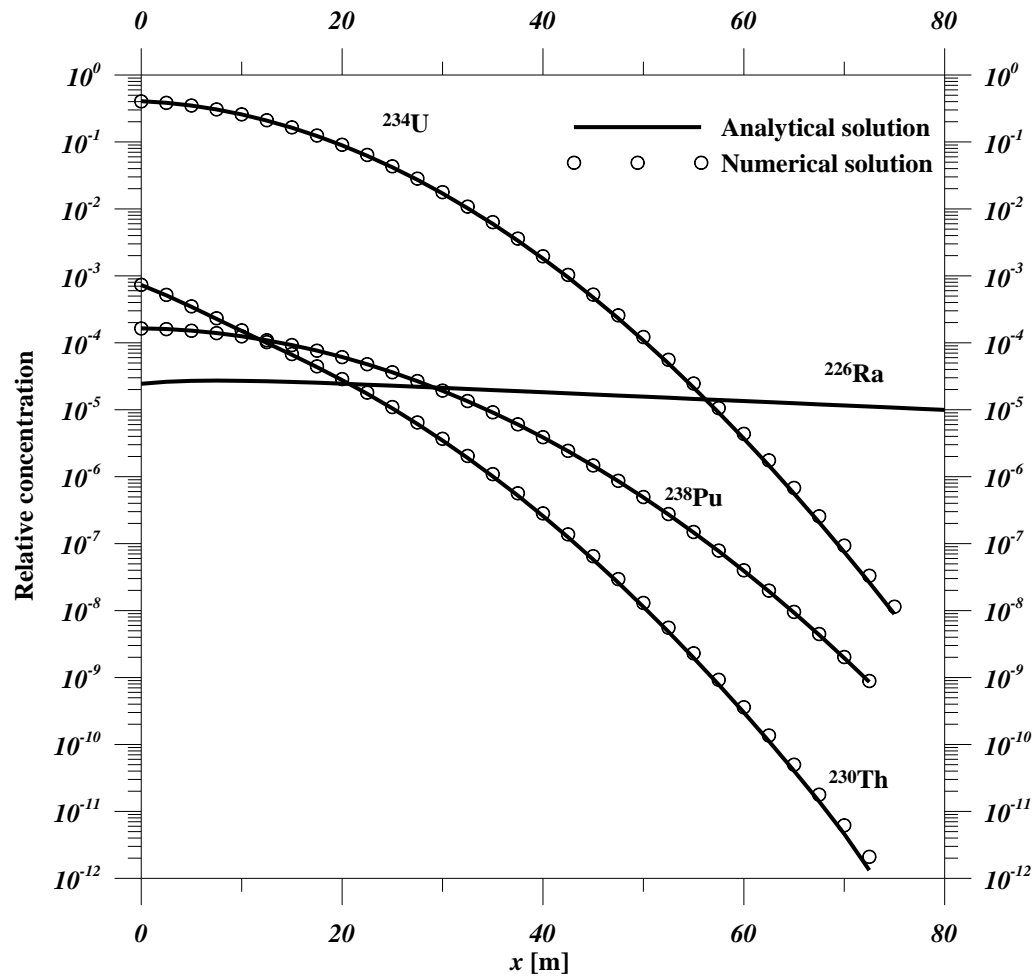


Fig. 2.

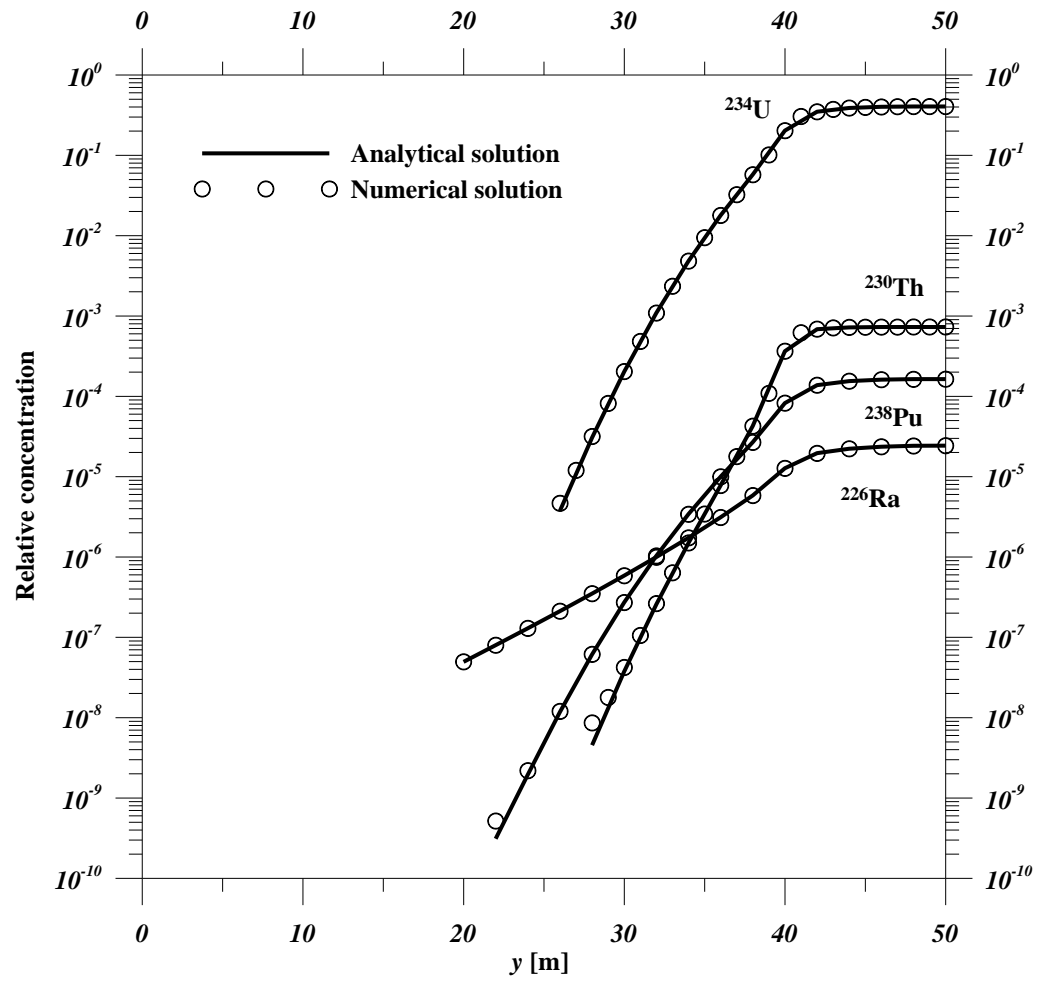


Fig. 3

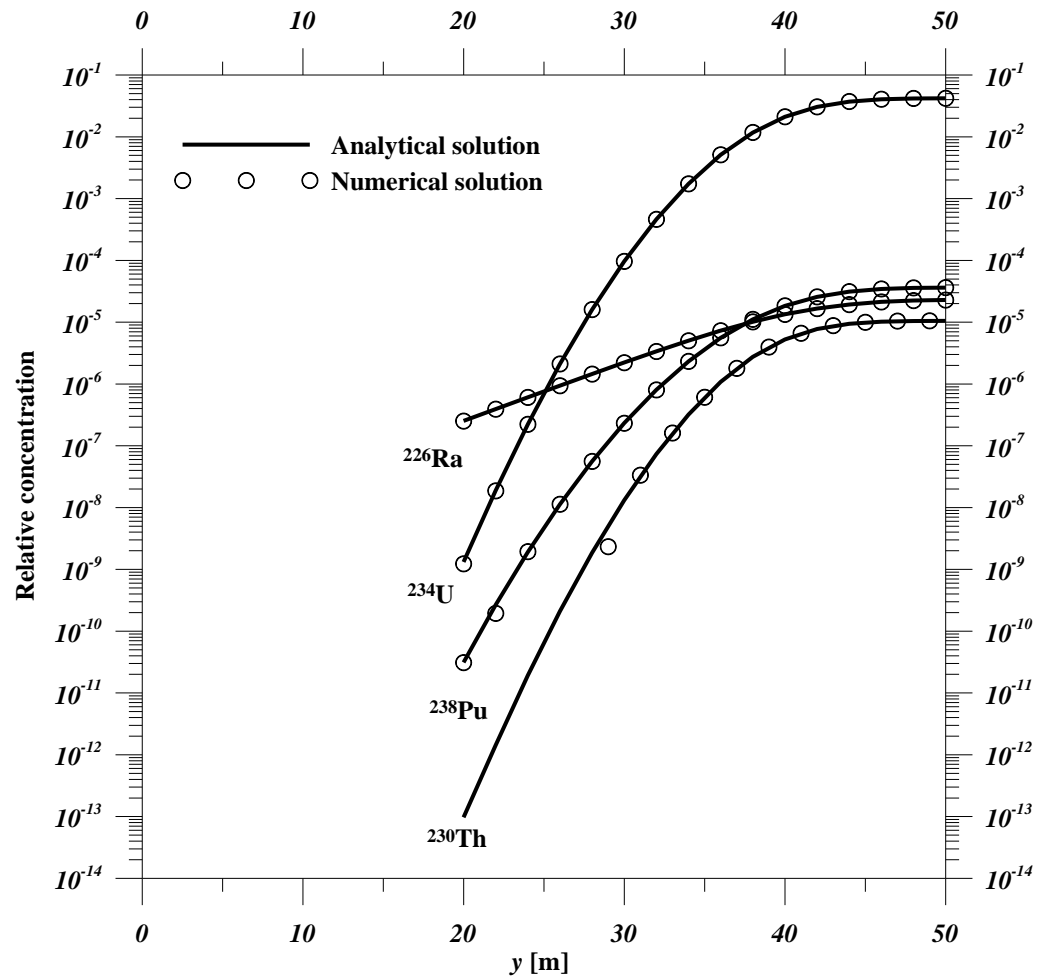


Fig. 4

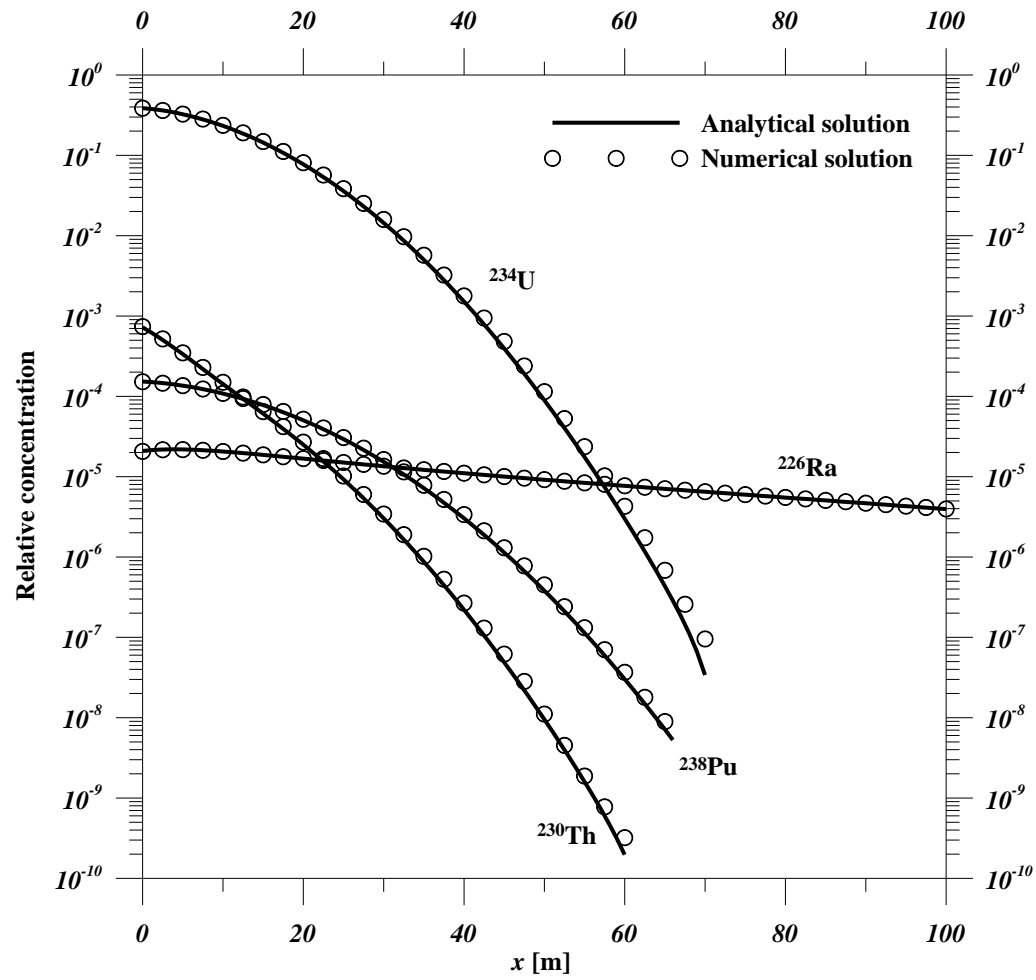


Fig. 5

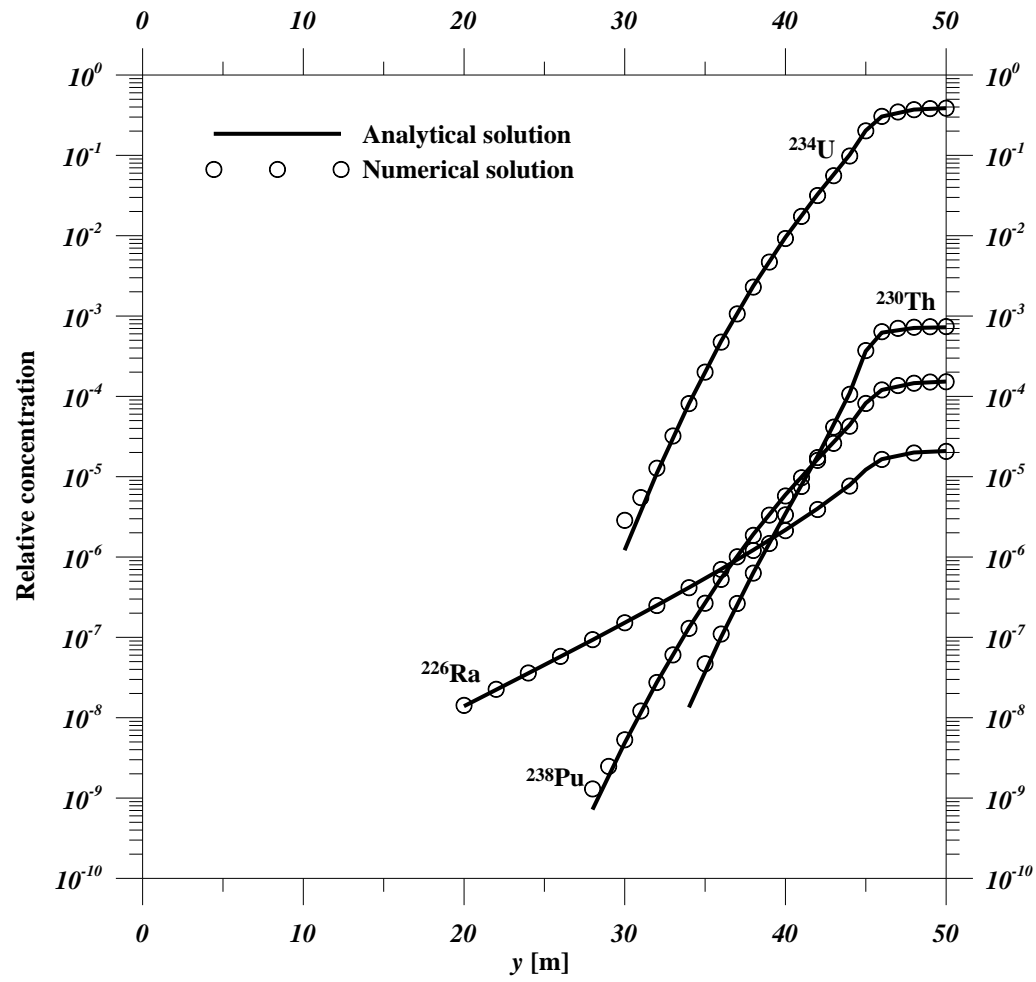


Fig. 6

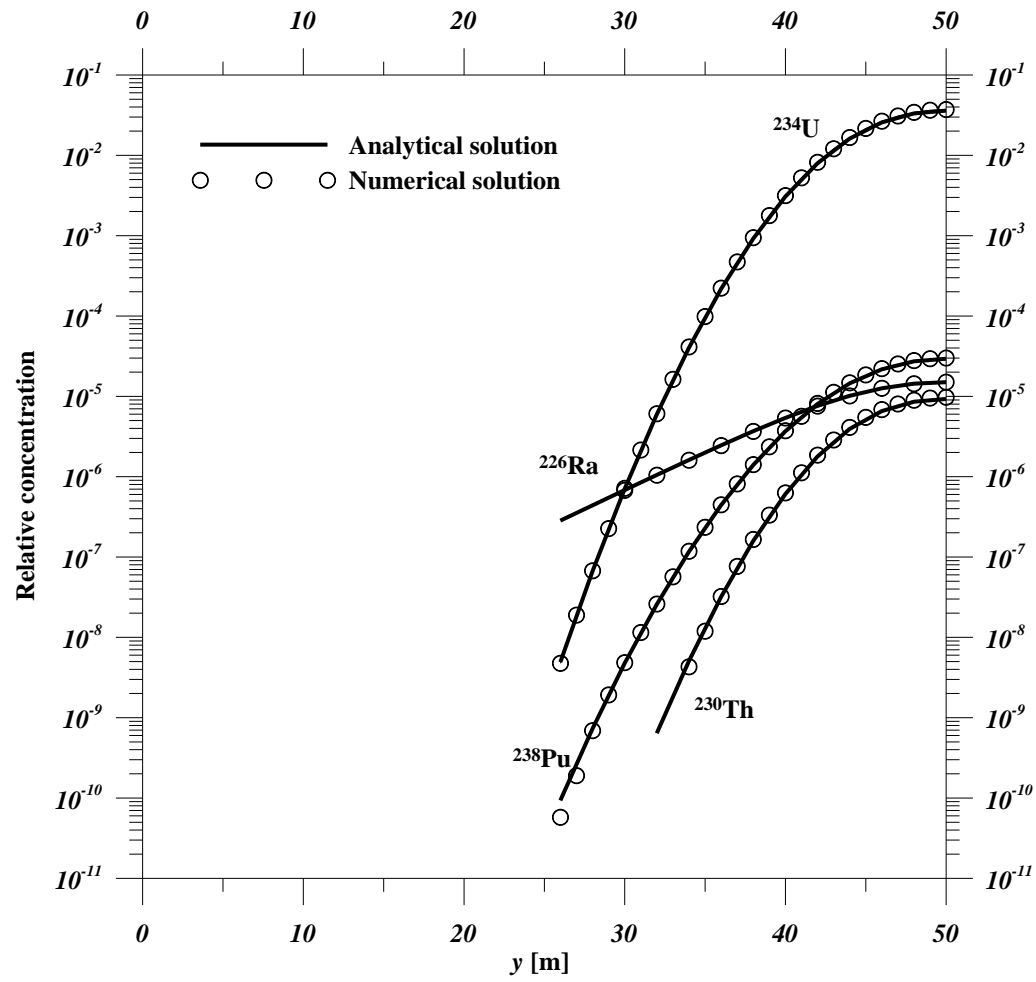


Fig. 7

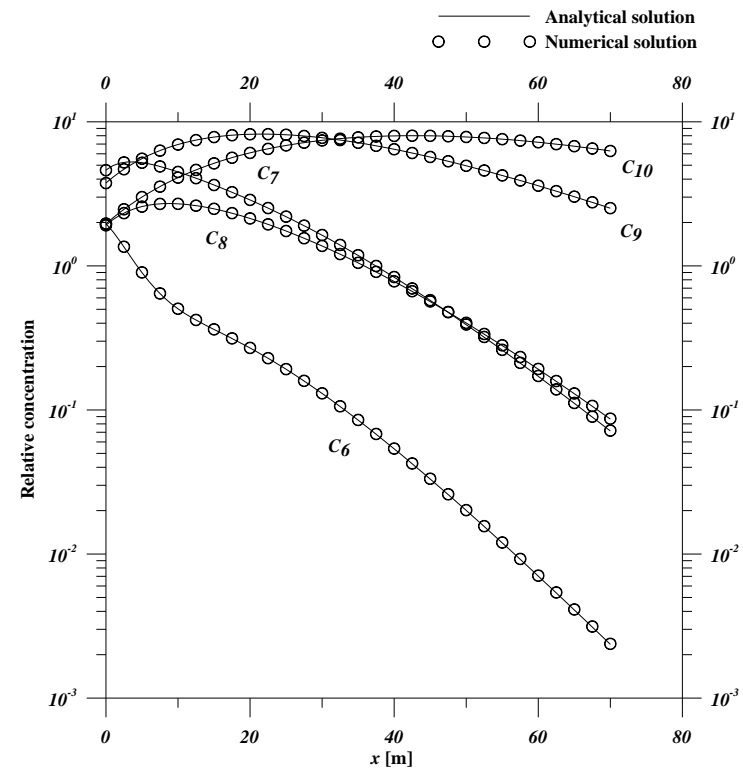
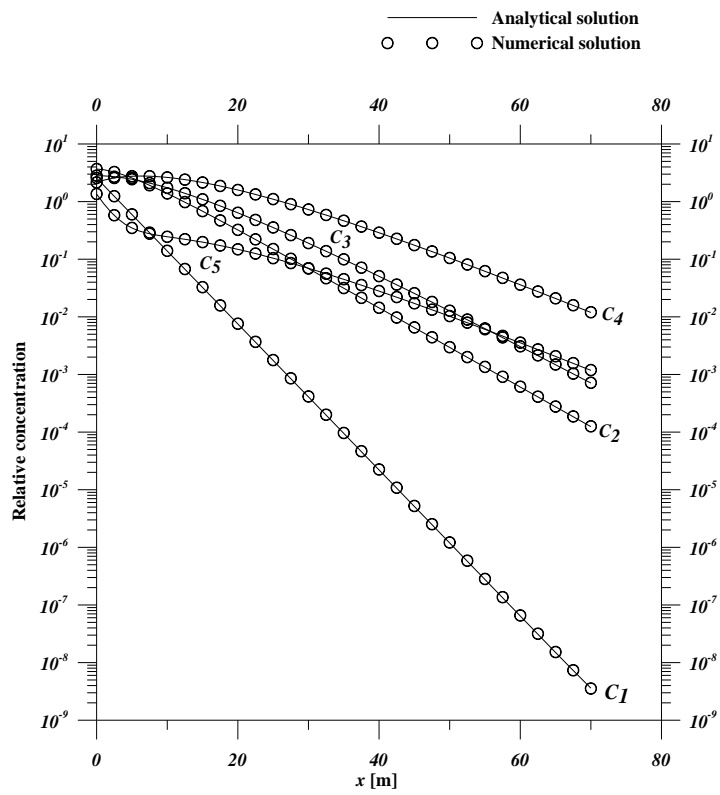


Fig. 8

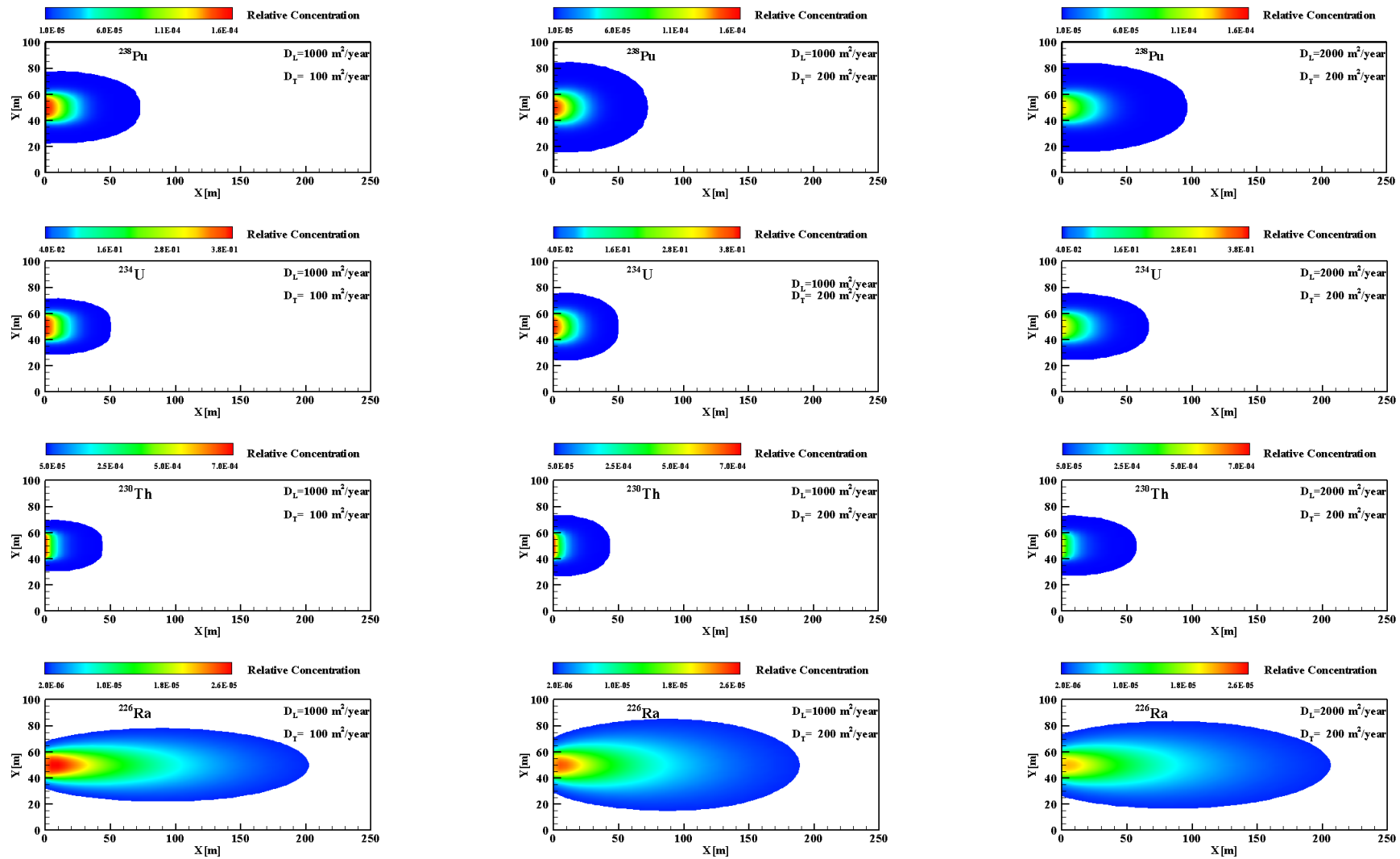


Fig. 9

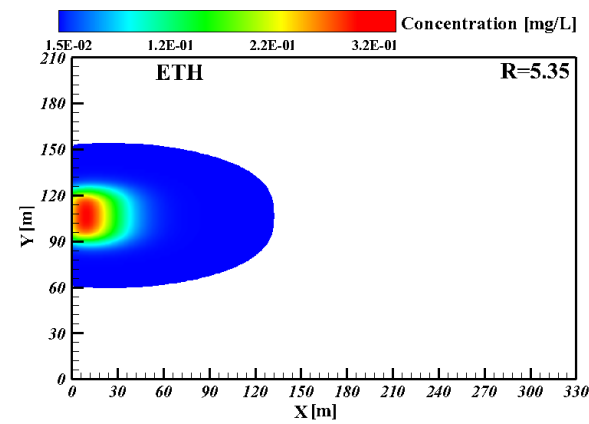
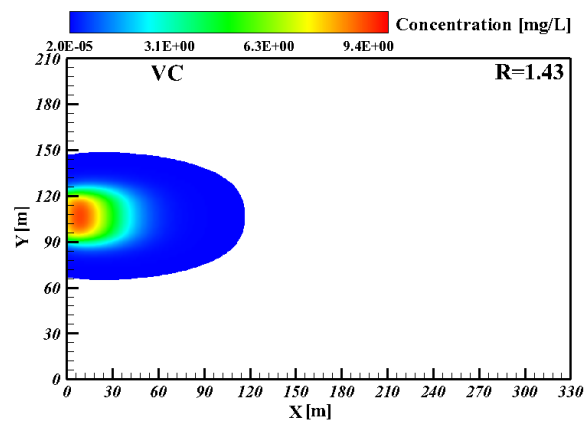
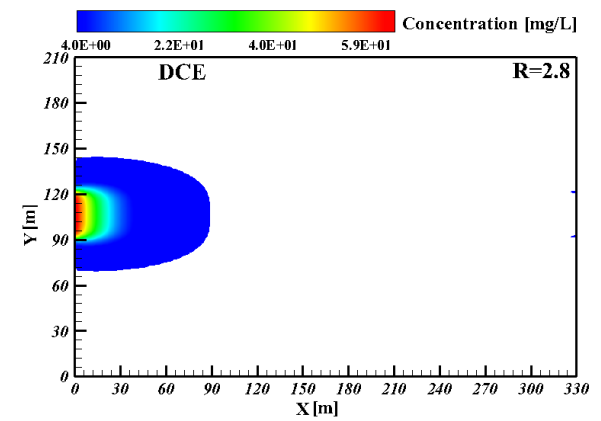
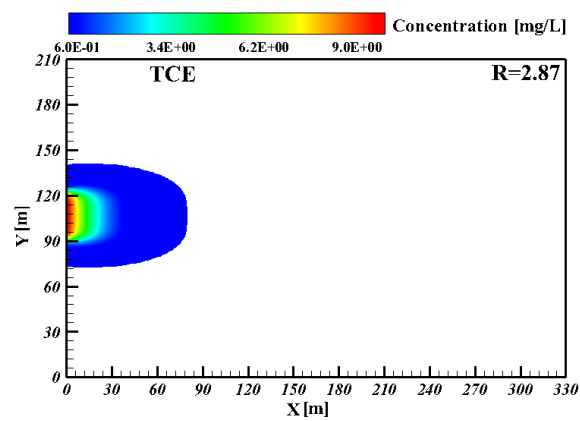
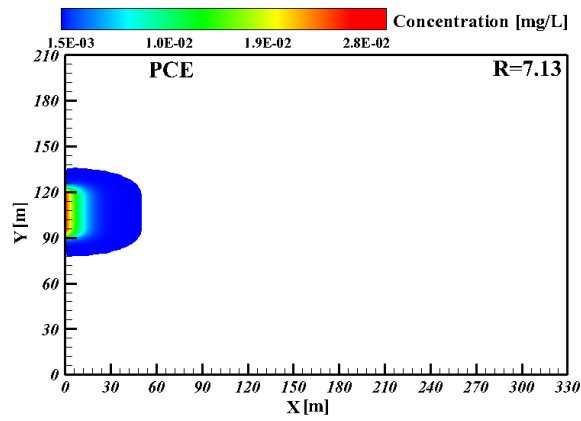


Fig. 10